STYRELSEN FÖR

VINTERSJÖFARTSFORSKNING

WINTER NAVIGATION RESEARCH BOARD

Research Report No 70

Juhani Hämäläinen

PLASTIC DEFORMATION SIMULATIONS OF PROPELLER BLADES

Finnish Transport Safety Agency

Finnish Transport Agency

Finland

Swedish Maritime Administration

Swedish Transport Agency

Sweden

Talvimerenkulun tutkimusraportit – Winter Navigation Research Reports
ISSN 2342-4303
ISBN 978-952-311-019-9

FOREWORD

In its report no 70, the Winter Navigation Research Board presents the outcome of the project on plastic deformation simulations of propeller blades. According to the Finnish-Swedish Ice Class Rules, 2008, a propeller blade of a ship operating in ice must fail at a load given in the ice class regulations. This force is placed on the propeller blade at distance of 0.8R from the blade root with 2/3 spindle arm from the leading/trailing edge of the propeller blade. In this study two typical propeller blades were modelled using finite element method (FEM) and the ultimate failure load was calculated at 0.8R with spindle arms of 1/3 and 2/3. These results were compared to analytically calculated ones.

The Winter Navigation Research Board warmly thanks Mr. Juhani Hämäläinen for this report.

Helsinki and Norrköping

June 2014

Jorma Kämäräinen

Finnish Transport Safety Agency

Peter Fyrby

Swedish Maritime Administration

Tiina Tuurnala

Finnish Transport Agency

Stefan Eriksson

Swedish Transport Agency

RESEARCH REPORT

VTT-R-07623-10

Plastic deformation simulations of propeller blades

Authors: Juhani Hämäläinen

Confidentiality: Public

Report's title	
Plastic deformation simulations of propeller blades	
Customer, contact person, address Finnish Transport Safety Agency (1031715-9) Po Box 320,FI-00101 Helsinki, Finland	Order reference
Project name Plastic deformation simulations of propeller blades	Project number/Short name 72608
Author(s) Juhani Hämäläinen	Pages 46
Keywords propeller, plastic, FEM, spindle arm	Report identification code VTT-R-07623-10

Summary

According to Ice Class Regulations 2008 of the Finnish Maritime Administration, a propeller blade of a ship operating in ice must fail at a load given in the ice class regulations. This force is placed on the propeller blade at distance of 0.8R from the blade root with 2/3 spindle arm from the leading/trailing edge of the propeller blade. In this study two typical propeller blades were modelled using Finite element method (FEM) and the ultimate failure load was calculated at 0.8R with spindle arms of 1/3 and 2/3. These results were compared to analytically calculated ones.

According to FEM results, the failure load calculation procedure of a propeller blade in Ice Class Regulations 2008 is accurate for skewed propeller blades, and there is no need to change the spindle arm from 2/3 to 1/3. For ice strengthened blades of large expanded blade area ratio the calculation procedure does not work. The analytical calculations give too high expected loads. Material properties affect significantly to the ultimate load values.

Confidentiality	Public

Espoo 8.12.2010

Written by	Reviewed by	Accepted by
Juhani Hämäläinen	Kai Katajamäki	Pekka Koskinen
Research Assistant	Senior Research Scientist	Technology Manager

VTT's contact address
Vuorimiehentie 5, P.O. BOX 1000, 02044 Espoo VTT

Distribution (customer and VTT)

Contents

1. Introduction

The Finnish Maritime Administration issued 12/2008 Ice Class Regulations for Ships operating in the Baltic Sea. The ultimate load resulting from propeller blade failure is specified in these regulations, [1], p. 38 formula 6.25 This study focuses on the behaviour of the propeller blade in failure and verifies the formula 6.25 using FEM[1]. The relevance of the load of the formula 6.25 is compared with the results obtained by commercial software Abaqus FEA version 6.9EF1. Especially the spindle arm for calculations of the extreme blade spindle torque arm is examined. According to [1] the spindle arm is taken as 2/3 of the distance between the axis of blade rotation and the leading/trailing edge at the 0.8R radius. Loaded areas are shown in Picture 1. The objective of this study was to find answers to following questions:

- Does the formula 6.25 lead to over dimensioning of the propeller blade and shaft line components?
- Can the spindle torque arm be reduced to 1/3?

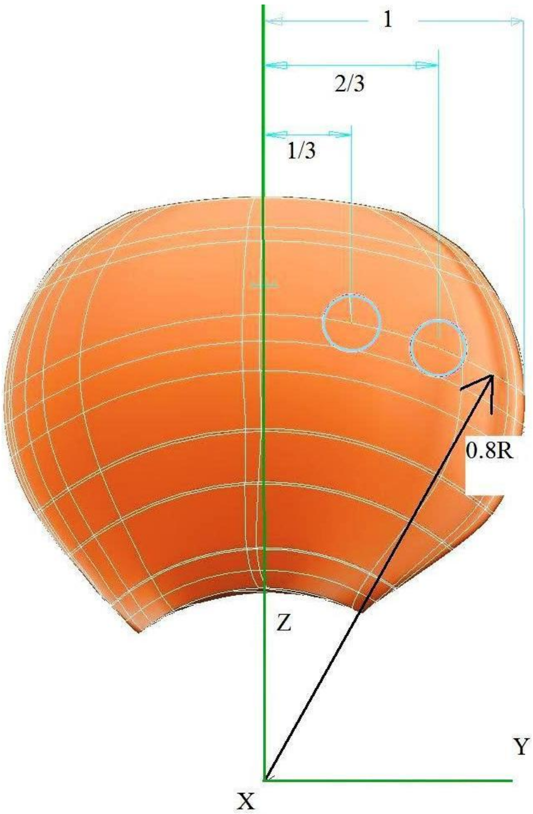

Picture 1, Loaded areas of the blade

[1] Finite Element Method (FEM) is a numerical technique for solving structural analysis problems.

2. Description

Two typical propeller types are examined. Blade of ship 1 in Picture 2 represents a skewed blade and the blade of ship 2 in Picture 3 represents an ice blade. Main dimensions of the blades and material properties used in the analysis are listed in the tables below. The strength values are the guarantee values.

Table 1, Blade data

Ship	**Blade type**	**Propeller diameter**	**Blade mass**	**Material**
Ship 1	Skew	4.06 m	968 kg (ρ=7850kg/m^3)	Steel
Ship 2	Ice Blade	2.00 m	192 kg (ρ=7580kg/m^3)	NiAl-Bronze

Table 2, Material data

Material	**Elastic Modulus, E [GPa]**	**Yield/ Ultimate strength [MPa]**	**Poisson constant**	**Elongation [%]**
NiAl-Bronze	123	235/650	0.33	19
Steel	200	520/650	0.3	15

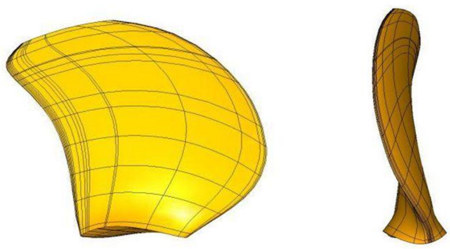

Picture 2, Ship 1 Skew blade

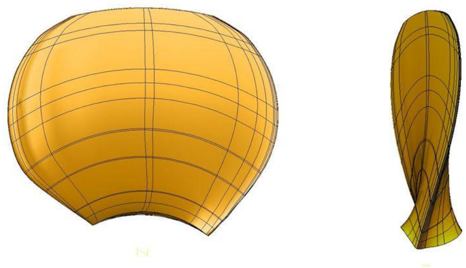

Picture 3, Ship 2, Ice blade

2.1. Analytical calculations – Ice class regulations propeller blade failure load

In Ice class regulations the propeller blade failure load calculation is described on page 26 and explained on pages 37-38. Definition of the load is shown in the table below.

Table 3, Propellerblade failure load definition, ref [1], p 26.

Notation	**Definiton**	**Use of the load in design process**
F_{EX}	Ultimate blade load resulting from blade loss through plastic bending. The force that is needed to cause total failure of the blade so that plastic hinge is caused to the root area. The force is acting on 0.8R. Spindle arm is to be taken as 2/3 of the distance between the axis of blade rotation and leading/trailing edge (whichever is the greater) at the0.8R radius.	Blade failure load is used to dimension the blade bolts, pitch control mechanism, propeller shaft, propeller shaft bearings and trust bearing. The objective is to guarantee that total propeller blade failure should not cause damage to other components.

2.1.1. Loading

According to the Ice Class Regulations 2008, the blade failure load is:

Formula 6.25:

$$F_{ex} := 300\frac{c_L \cdot t^2 \cdot \sigma_{ref}}{0.8 \cdot D - 2r}$$

where:
D = propeller diameter
t = root section thickness
r = root section radius
c_L= root section length
$\sigma_{ref} = 0.6\sigma_{0.2} + 0.4\sigma_u$

t, r and c_L are to be taken at the weakest section of the blade outside the root fillet. For ship 1 the cross section geometry of the blade was projected at various radius on a plane and the needed variables were measured. For ship 2 needed values were taken from actual workshop drawings.

2.1.2. Load cases

The propeller blades are studied using three different load cases. Load case 1 is conducted by ice class regulations 2008. Load case 2 is a proposal for alternative calculation of blade failure load. Load case 3 is considered in detail in results section. In general this load case was made to make the ice blade deform plastically at the root section.

Table 4, Load cases

Load case	applied area	description
1	2/3 of the distance between the axis of blade rotation and the leading/trailing edge at the 0.8R radius	Ice Class Regulations Blade failure load 6.25
2	1/3 of the distance between the axis of blade rotation and the leading/trailing edge at the 0.8R radius	Proposal for new loading area
3	A pressure on a surface from 0.7R to 0.9R	For ship 2 ice blade; to find the ultimate shaft propeller bending moment.

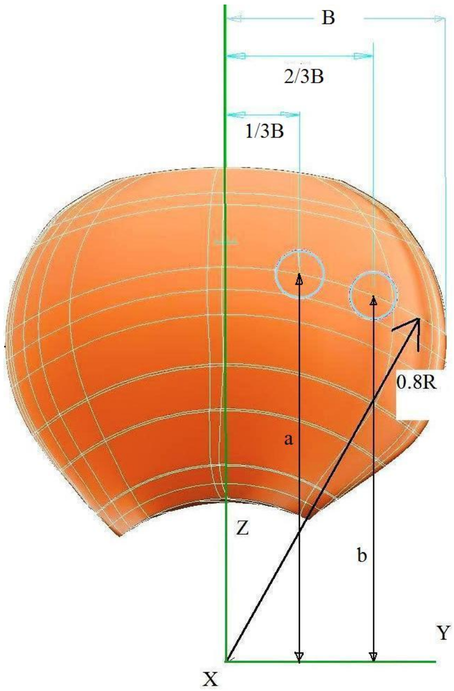

Picture 4, Loaded areas

2.1.3. Analytical failure loads and torques

According to Ice class regulations 2008 formula 6.25 the failure forces were calculated as described in section 2.1.1. By iteration the lowest failure load was found at 0.5R on both blades. Below mentioned quantities were used to calculate the failure load for each blade.

Analytical moments M_Y and M_Z were calculated to show the effect of the failure load at the propeller shaft and hub. The ice class regulations 2008 give no specification for calculation of these moments and they are made only for illustrative purposes for this study. M_Y moment arms a and b and M_Z moment arms 1/3B and 2/3B in Picture 4 are held constant. The analytically calculated failure loads and moments for specified load case are shown in Table 5.

Quantities for calculation - Skewed blade

Propeller diameter	D = 4.058	m
R0.5 root section thickness	t = 0.113	m
R0.5 root section radius	r = 1.014	m
R0.5 root section length	c_L =1.165	m

Quantities for calculation - Ice blade

Propeller diameter	D = 1.99	m
R0.5 root section thickness	t = 0.082	m
R0.5 root section radius	r = 0.497	m
R0.5 root section length	c_L = 0.786	m

Table 5, Reference loads and moments, A

Blade, Load Case	**Force F_{ex} [MN]**	**Bending M_Y[MNm]**	**Spindle M_Z[MNm]**
Skew, Load case 1	2.10	3.18	1.23
Skew, Load case 2	2.10	3.35	0.61
Ice, Load case 1	1.04	0.77	0.31
Ice, Load case 2	1.04	0.82	0.16
Ice, Load case 3	1.04	0.83	0

Where:
F_{ex}= blade failure load by [1], p.38 fomula 6.25
M_Y= analytical propeller shaft bending moment with constant moment arm a and b, see Picture 4
M_Z= analytical spindle moment with constant moment arm 1/3B or 2/3B specified by the load case, see Picture 4

3. Limitations

For ship 1 the measures used to calculate the ultimate blade failure load are taken from CAD models of the propeller blades, not from the actual workshop drawing. Thus minor error is evident, due to projection of the propeller cross-section etc. This has no effect on the magnitude of the strength of the blade.

The Abaqus material model is a bilinear stress strain curve with isotropic hardening effect. This is a simplification from the actual elastic-plastic model of metal materials. The elastic modulus of both materials is estimated to match typical values of the specific material. Other material data originates from actual workshop data of the blades.

4. Finite element analysis

Finite element analysis was made with FEA Software Abaqus version 6.9 EF1. EF1 (Extended functionality 1) is a verified version of Abaqus with some extended functionalities to standard 6.9 version. These extension are not used in this study and do not affect the results.

4.1. Meshing and mesh quality

The propeller blades were discretized with parabolic ten-noded tetrahedral elements, Abaqus notation C3D10. This element is capable of following the complex geometry of the blades. The performance of this element is studied in appendix A. Plastic deformation was estimated to occur at the root section, thus 8-12 elements over thickness of the blade were used from the root of the blade to radius 0.5R. An average relative element size of 10-15mm was used on both models. All in all three different FE-models were made. VTT's in-house quality check procedures for finite element models and software were used in this study in order to ensure accurate modelling results.

4.1.1. Loading and boundary conditions

In the FE-models the loading is applied as a pressure on an area specified by the load case. In load cases 1 and 2 the loaded are is a circular area diameter of witch is 10% of the blade radius. In the load case 3 loaded area is bound between 0.7R to 0.9R. Loaded areas are shown in Picture 1 and Picture 4. The pressure acts in the direction of the blade surface normal and so it follows the deformation of the blade, this is regarded in the results. Calculation is force driven, and the pressure is gained until blade failure and beyond to see post failure behaviour of the blade.

In CAD environment the origin of the global coordinate system was placed at the propeller shaft centre of rotation (COR). Coordinate system orientation is shown in Picture 5. The global x-axis is parallel and coincident with the propeller shaft axis. The global z-axis is parallel and coincident with the blade turning axis. All coordinate directions in this report refer to global coordinate axes.

Propeller shaft was modelled with rigid element. The roots of the blades were rigidly bound to the global origin at the shaft COR. Boundary conditions are illustrated in Picture 6. Reaction forces and moments were printed at the COR.

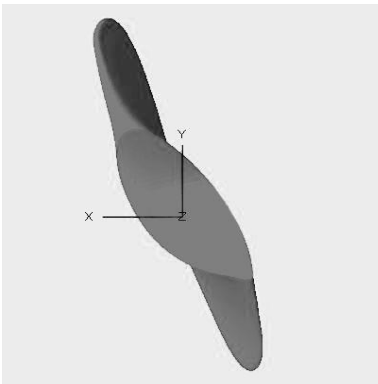

Picture 5, Coordinate system

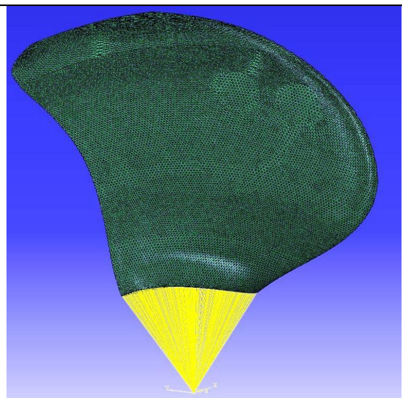

Picture 6, Boundary conditions

4.2. Studied cases

Four different cases are discussed in this study. These are:

1. Skewed blade failure load analysis
2. Ice Blade failure load analysis
3. Material property validation
4. Element type validation, see Appendix A

5. Results

The propeller blades were calculated with their original materials in all load cases. In section 5.3 the materials were changed and the blades were calculated again. According to section 4.1.1 the orientation of the applied pressure changes as the blade deforms. Thus only F_X reaction force components are shown in the displacement – reaction force plots. A resultant reaction force would give too high failure load values. Other force components are regarded as secondary for the strength of the blade. Displacement of the blade is given the as resultant of the displacement components at the most deflected area of the blade.

For example graphs in Picture 8 and Picture 12 illustrate the total displacement of the propeller blade end tip versus reaction force at the shaft spinning axis COR. The red line shows the failure load given by formula 6.25 in [1]. Total displacement versus moment plots are made to illustrate loadings on the propeller shaft and components related to the propeller hub. In moment plots Picture 9 and Picture 13 for example horizontal lines show the maximum bending moments calculated analytically from failure load. M_Y is the bending around the global y-axis. This quantity represents propeller shaft bending. M_Z is bending moment around the global z-axis, this quantity represent spindle moment.

5.1. Ship 1

The deformation and the plastic behaviour of ship 1 is briefly shown in Picture 7. Load case 1 behaviour is seen in the left hand column, for load cases see Table 4. Right hand side column illustrates load case 2 behaviour respectively. Plastic area size at failure was observed by relation of elements with plastic strain to total amount of elements in the model.

5.1.1. Load case 1

Pictures 7A and 7B show the total deformation of the blade at failure load. Dashed geometry represent the initial shape of the propeller. Pictures 7C and 7 D illustrate the area of plastic deformation at failure load. Solid blue line in Picture 8 represents the result of load case 1. Reaction moments M_Y and M_Z are presented in Picture 9. Some values at failure are gathered in Table 6.

At failure two areas of plastic deformation can bee seen, picture 7C. These result from simultaneous bending in YZ-plane and twisting around Z-axis. In general the plastic area occurs in the root section of the blade, below 0.5R. Once maximum failure load is achieved, the plastic deformation propagates in the upper plastic area, pictures 7E and 7F. Reaction force at failure achieves maximum value about 16% below the analytical blade failure load. The reaction force reduces gradually after the maximum value. The maximum propeller shaft bending moment M_Y is about 10% lower than could be expected by analytical calculations, see Table 5. The maximum propeller blade spindle moment M_Z is about 3% higher than expected by analytical calculations. In load case 1 the analytical calculations give good approximations for the propeller blade failure loads.

5.1.2. Load case 2

Load response of the blade is shown in Picture 8 by a dashed blue line and Picture 10 illustrates reaction moments.

In load case 2, the propeller blade behaviour is very similar to load case 1, see right hand column in Picture 7. The plastic area appears more horizontal than in load case 1 and its size is 5 percentage units smaller, see Table 6. The ultimate failure load is about 3% lower than analytically calculated. The maximum propeller shaft bending moment M_Y is about 4% lower than expected by analytical calculations. The maximum propeller blade spindle moment M_Z is 24 % higher than expected. Analytical calculations under estimate the actual spindle moment but are able to estimate propeller shaft bending.

Table 6, Ship 1 plastic area size at failure

Blade, Load case	**Plastic elem./total elem.**	**Plastic elements [%]**	**Force RF_{max} /Fex**	**Force [%]**	**Bending RM_Y/ M_Y**	**Bending [%]**	**Spindle RMz/ Mz**	**Spindle [%]**
Skew, Load case 1	88499/254300	34.0 %	1.975/2.10	94.2%	2.87/3.18	90.2%	1.29/1.23	102%
Skew, Load case 2	73789/254300	29.0%	2.034/ 2.10	96.9%	3.22/3.35	96.2%	0.76/0.61	124%

where:
Plastic elem. = Number of plastic elements at failure load, plasticity limits [0.5%-6%]
Total elem. = Number of total elements in the FE-model
RF_{max} = Maximum reaction force in Picture 8
RM = Maximum reaction moments in Picture 9 and Picture 10
M_Y = analytical moment, Table 5
M_Z = analytical moment, Table 5
Fex = Blade failure load, Table 5

<table>
<tr><th>Load case 1, Force at 2/3 spindle arm</th><th>Load case 2, Force at 1/3 spindle arm</th></tr>
<tr><td>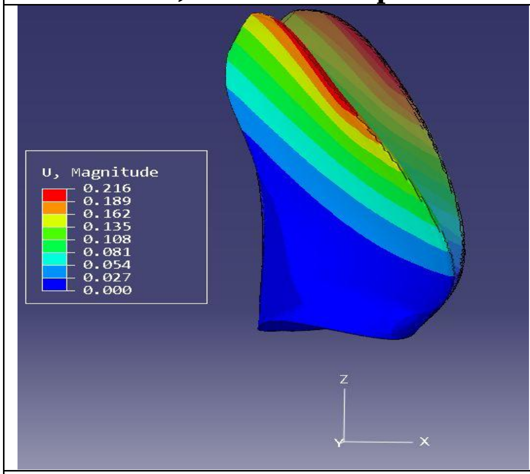
</td><td>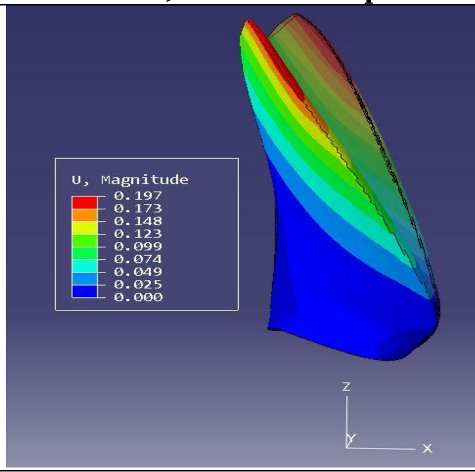
</td></tr>
<tr><td>A: Displacement U≈200mm at failure</td><td>B: Displacement U≈200mm at failure</td></tr>
<tr><td>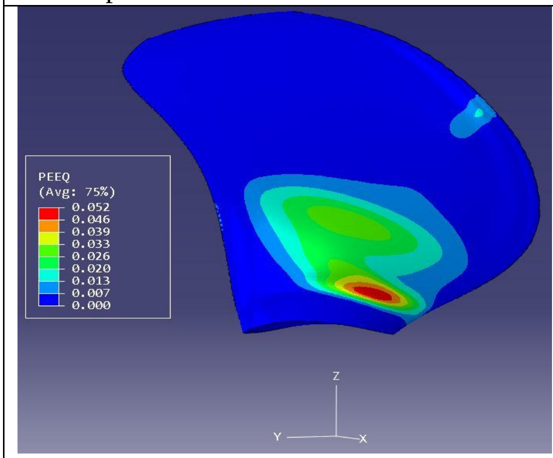
</td><td>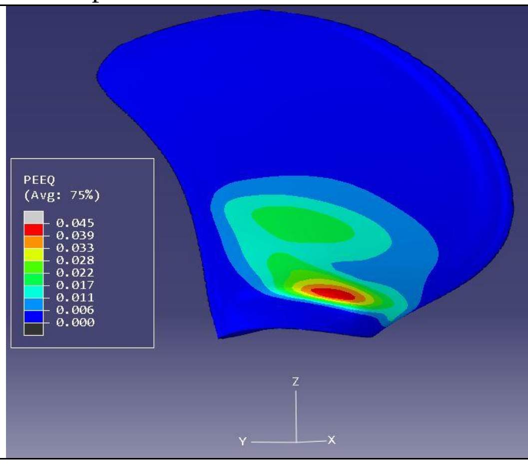
</td></tr>
<tr><td>C: Plastic strain at failure, U≈200mm, Max strain ≈5.2%</td><td>D: Plastic strain at failure, U≈200mm, Max strain≈4.5%</td></tr>
<tr><td>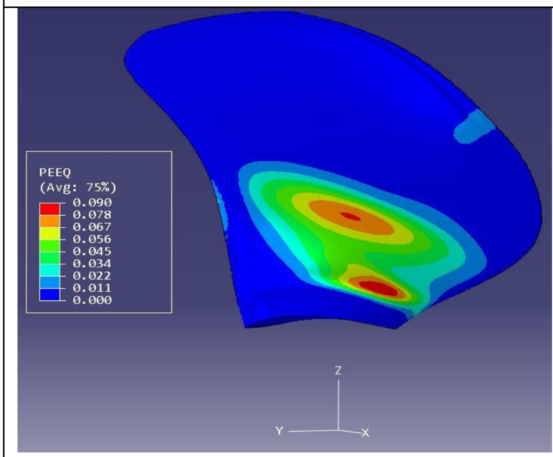
</td><td>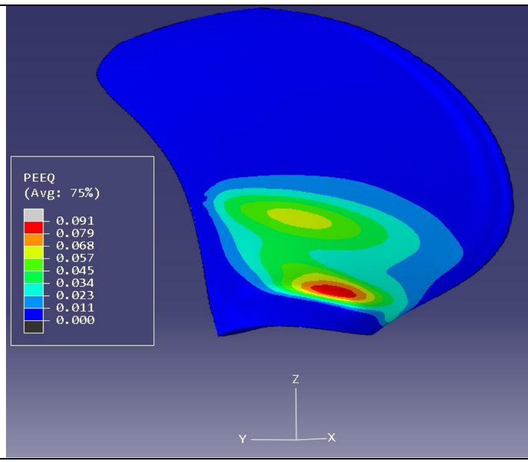
</td></tr>
<tr><td>E: Plastic strain propagation, U≈400, Max strain ≈9.0%</td><td>F: Plastic strain propagation U≈400, Max strain ≈9.1%</td></tr>
</table>

Picture 7, Ship 1 Blade behaviour at loading

5.1.3. Ship 1 Plots

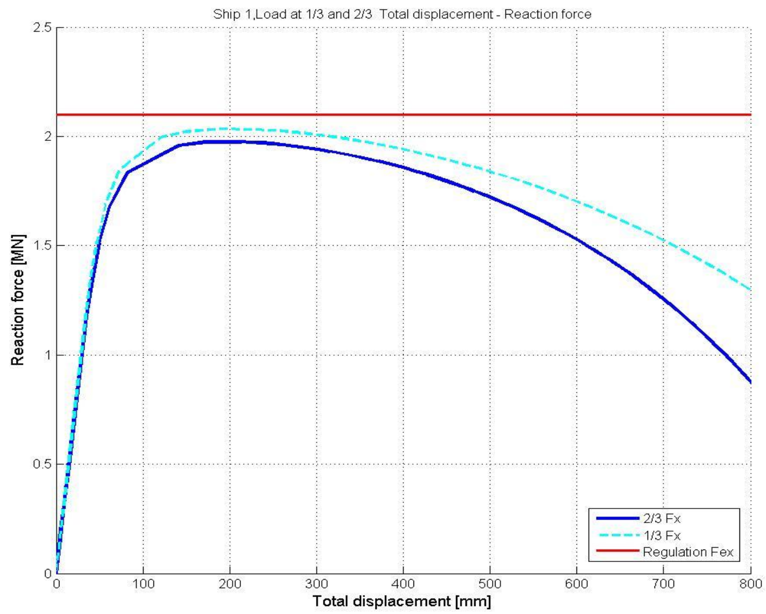

Picture 8, Ship response, blade force versus blade tip displacement

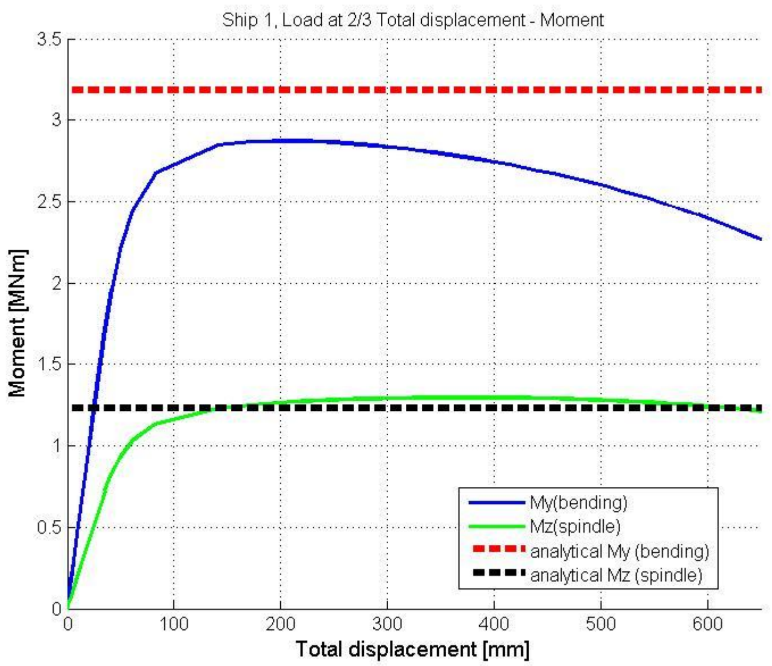

Picture 9, Ship 1, moments versus blade tip displacement, load case 1

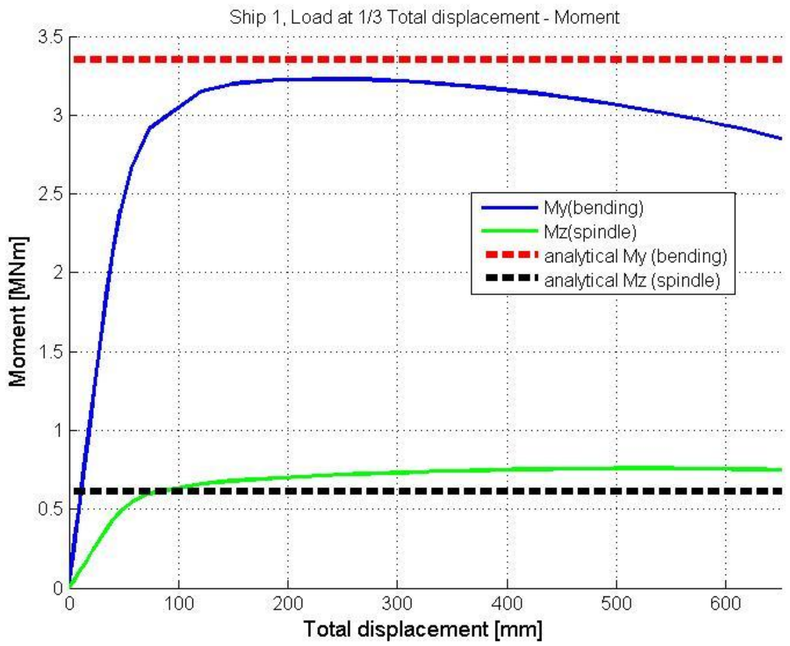

Picture 10, Ship 1, moments versus blade tip displacement, load case 2

5.2. Ship 2

Propeller of ship 2 has equal distances from leading/trailing edge to turning axis of the blade (global z-axis). Thus calculations had to be made on both edges of the blade.

5.2.1. Load case 1, leading edge

In Picture 11 C plastic zone of the blade is shown and 11 A illustrates blade deflection. In general the plastic area expands over the radius of the blade and its principal axis is not horizontal. Once maximum failure load is achieved, the plastic deformation does not propagate in other areas and no further pictures are needed to illustrate the post failure behaviour of the blade. Plastic area size is considered in Table 7.

Solid blue line in Picture 12 represents the result of load case 1. This load achieves maximum value about 47% under the analytical blade failure load, see Table 5. Reaction moments M_Y and M_Z are presented in Picture 13. The maximum propeller shaft bending moment M_Y is about 50% lower than could be expected by analytical calculations. The maximum propeller blade spindle moment M_Z is about 45% lower than expected. At failure almost 50% of the FE-model elements show plastic deformation, Table 7. Analytical calculations are not able to predict the blade failure load for the ice blade in load case 1.

5.2.2. Load case 2, leading edge

In Picture 11 D the plastic zone can be seen and 11 B illustrates blade deflection. The plastic area expands over the radius of the blade and its principal axis is not horizontal. Size of the plastic area is bigger than in load case 1, Plastic area size is considered in Table 7.

Dashed light blue line in Picture 12 represents the force response of load case 2. Reaction force achieves maximum value about 68% of the analytical blade failure load. The reaction force reduces gradually after the maximum value. Reaction moments M_Y and M_Z are presented in Picture 14. The maximum propeller shaft bending moment M_Y is about 33% lower than expected by analytical calculations. For analytical calculations see section 2.1. Maximum propeller blade spindle moment M_Z is about 12% lower than expected. At failure most of the FE-model elements show plastic deformation, Table 7. Analytical calculations are not able to predict failure load for the ice blade in load case 2. Analytically calculated spindle moment and reaction spindle moment are close.

Table 7, Ship 2 Plastic area at failure

Blade, Load case	**Plastic elem./ total elem.**	**Plastic elements [%]**	**Force RF_{max} / Fex**	**Force [%]**	**Bending RM_Y/ M_Y**	**Bending [%]**	**Spindle RMz/ Mz**	**Spindle [%]**
Ice, Load case 1	105308/217883	48.3%	0.555/1.044	53.2%	0.39/0.77	50.6%	0.17/0.31	54.8%
Ice, Load case 2	143998/217883	66.0%	0.713/1.044	68.3%	0.55/0.82	67.1%	0.14/0.16	87.5%

where:
Plastic elem. = Number of plastic elements at failure load, plasticity limits [0.5%-10%]
Total elem. = Number of total elements in the FE-model
RF_{max} = Maximum reaction force in Picture 12
RM = Maximum reaction moment in Picture 13 and Picture 14
Fex = Blade failure load, Table 5
M_Y = analytical moment, Table 5
M_Z = analytical moment, Table 5
Fex = Blade failure load, Table 5

<table>
<tr><th>LOAD CASE 1, Force at 2/3 spindel arm</th><th>LOAD CASE 2, Force at 1/3 spindel arm</th></tr>
<tr><td>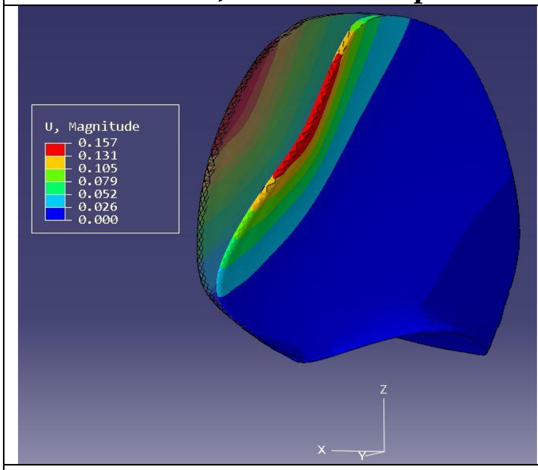
</td><td>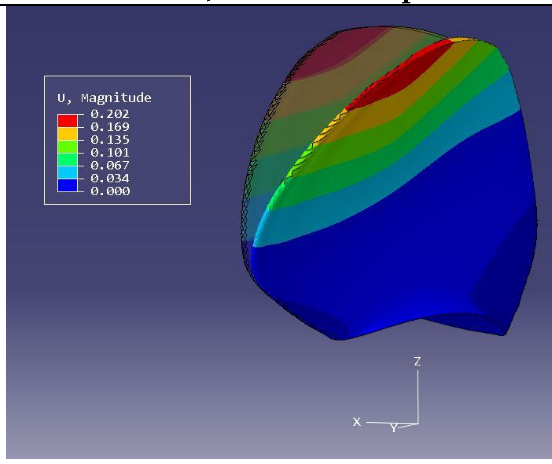
</td></tr>
<tr><td>A: Deformation at failure, U_{max}=157mm</td><td>B: Deformation at failure, U_{max}=202mm</td></tr>
<tr><td>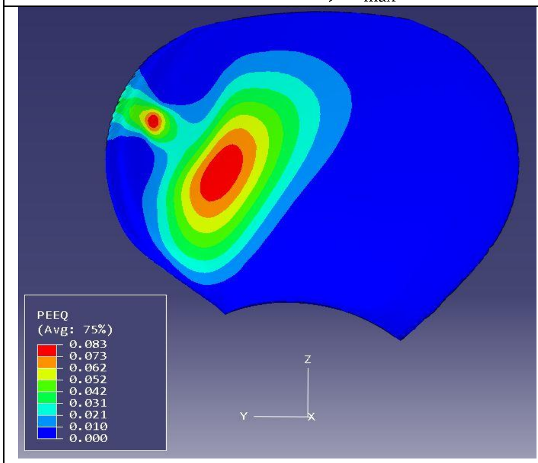
</td><td>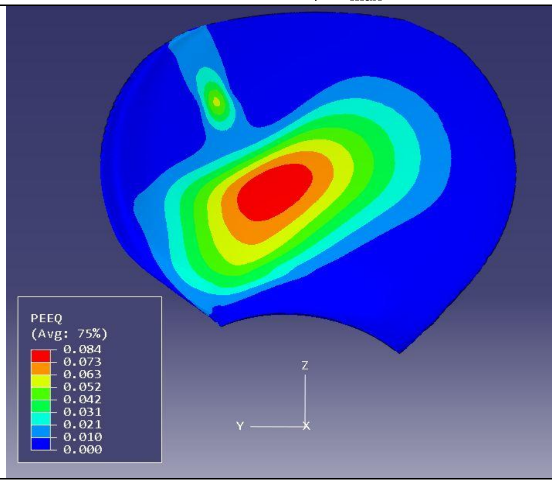
</td></tr>
<tr><td>C: Plastic strain at failure, U_{max}=157mm, Max strain =8.3%</td><td>D: plastic strain at failure U_{max}=202mm, Max strain =8.4%</td></tr>
</table>

Picture 11, Ship 2 propeller blade behaviour under loading

5.2.3. Ship 2 Plots

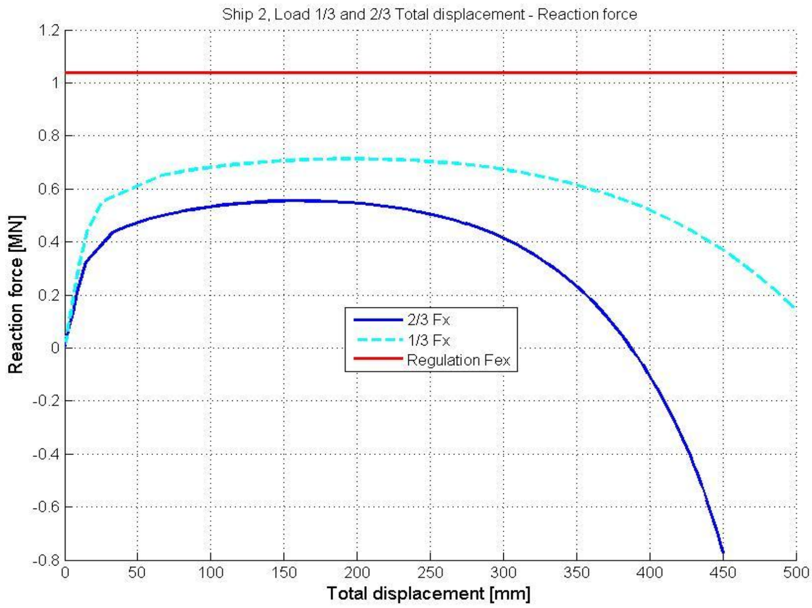

Picture 12, Ship 2 Total end tip displacement (U) - Reaction force

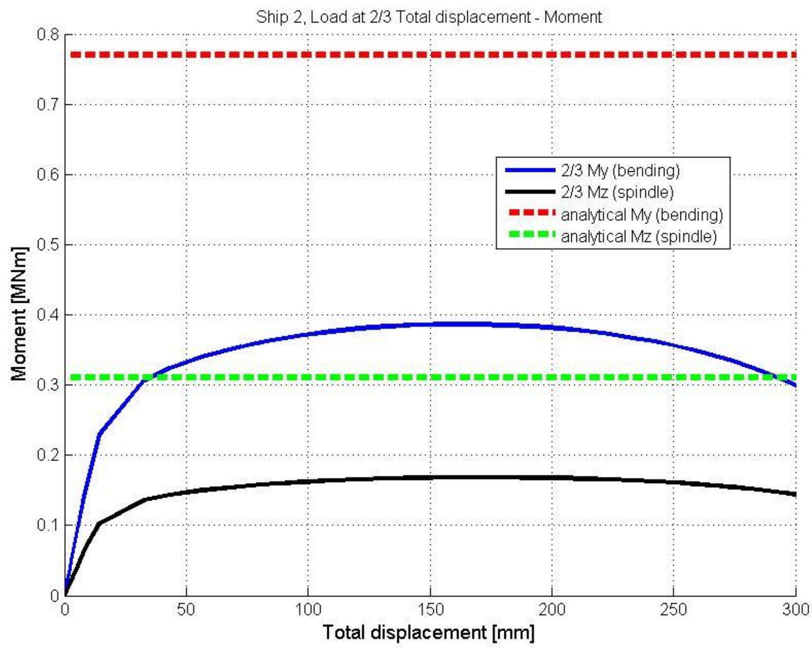

Picture 13, Ship 2 Reaction moments

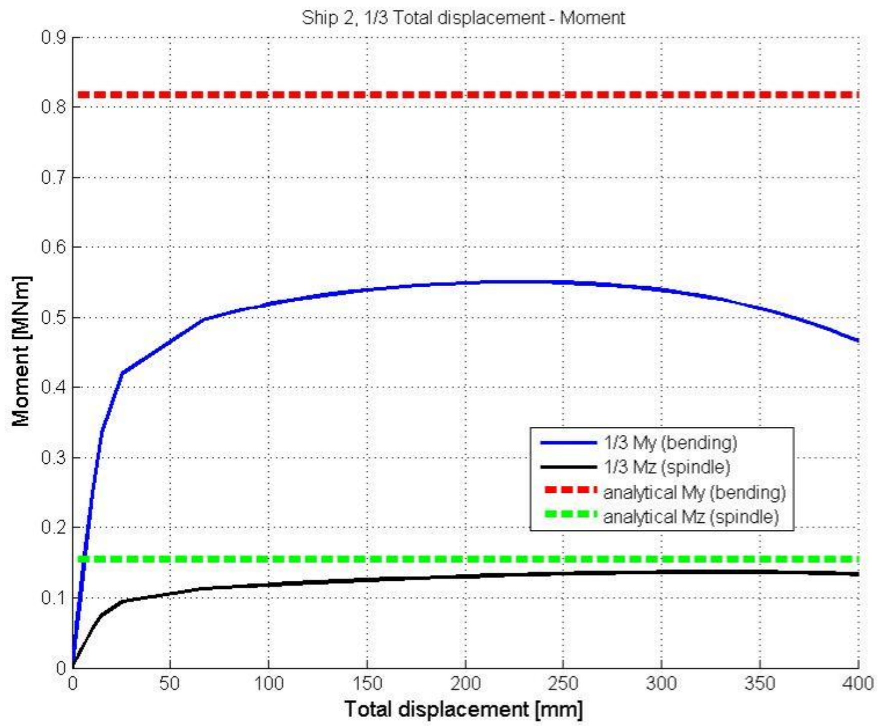

Picture 14, Ship 2, Reaction moments, load case 2

5.2.4. Load at trailing edge

Loads at trailing edge of the propeller blade were studied in load cases 1 and 2. The load responses of load cases 1 and 2 are shown in Picture 16 and Picture 17. These pictures shows that the loads applied to trailing edge of an ice blade result very low loads on the propeller shaft. As the bending force on the shaft is smaller than in calculations for leading edge, no moment plots for trailing edge are discussed; the reaction moments of these plots would be left way behind expected.

Plastic strain at failure is illustrated in Picture 15. In Picture 15 A load case 1 plastic zone at failure load occurs in the upper right hand side corner of the blade distance away from root section of the blade. At failure only a small amount of plastic deformation has occurred and the plastic zone is very local. In Picture 15 B load case 2 plastic deformation occurs on a bigger area than in load case 1, but this deformation is still very local. Pictures 17 C and D show that after failure plastic deformation propagates at the initial plastic area. Analytical calculations are not able to predict ice blade failure load at the trailing edge of the blade.

<table>
<tr><th>Load case 1, TRAILING EDGE 2/3</th><th>Load case 2, TRAILING EDGE 1/3</th></tr>
<tr><td>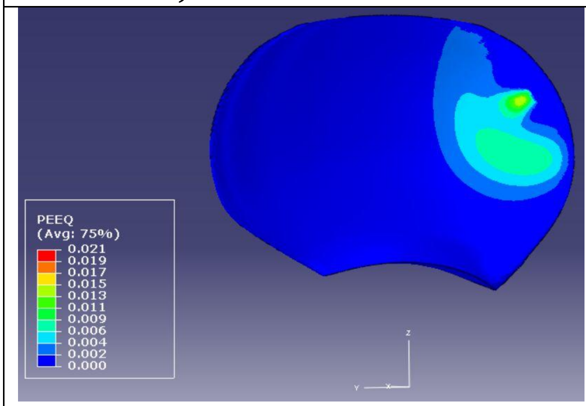
</td><td>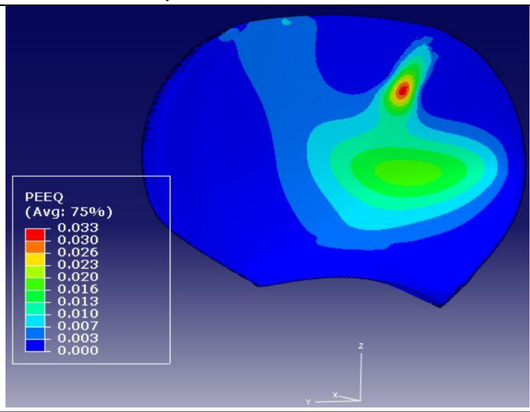
</td></tr>
<tr><td>A: Plastic strain at failure, U_{max}=28mm, Max strain =2.1%</td><td>B: Plastic strain at failure U_{max}=58mm, Max strain =3,3%</td></tr>
<tr><td>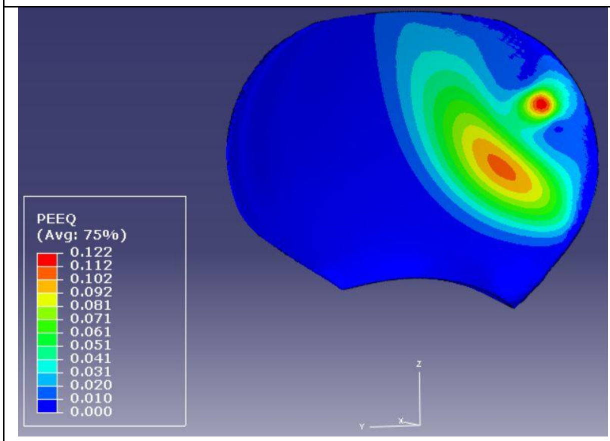
</td><td>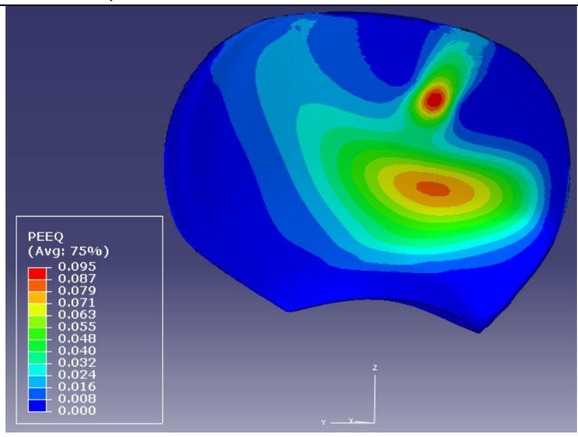
</td></tr>
<tr><td>C: Plastic strain after failure, U_{max}=209mm, Max strain =12%</td><td>D: plastic strain after failure U_{max}=205mm, Max strain =9.5%</td></tr>
</table>

Picture 15, Ship 2 Loading at trailing edge

5.2.5. Trailing edge, plots

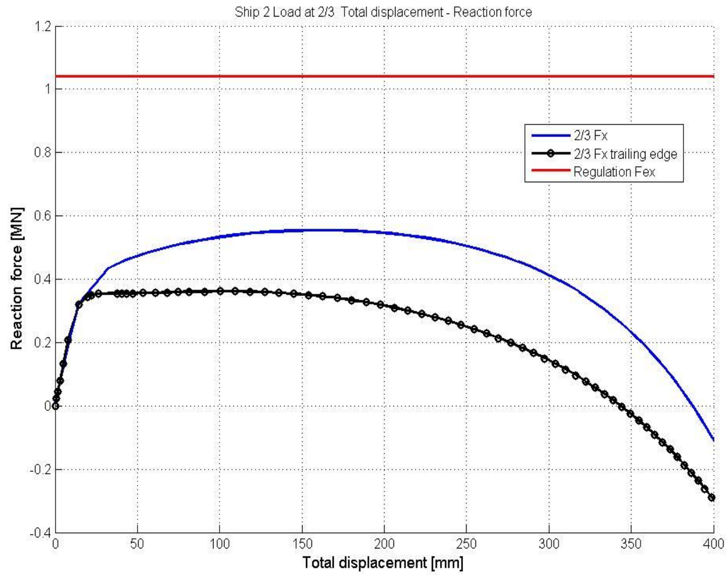

Picture 16, Ship 2, Reaction at leading/trailing edge

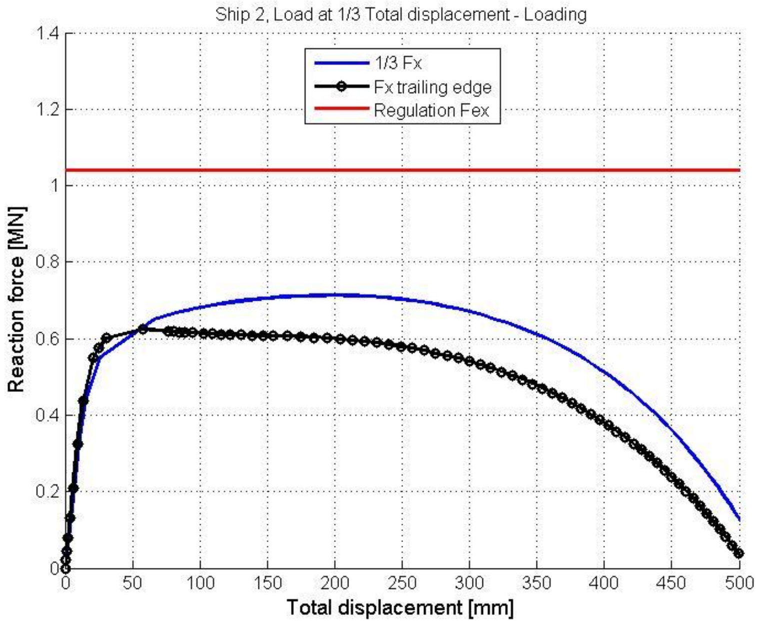

Picture 17, Ship 2 Reaction at leading/trailing edge 1/3 spindle

5.2.6. Load case 3

As in the other load cases the plastic area due to bending was not found in the root section of the blade of ship 2 an additional load case was defined. A pressure is applied on the area from R0.7 to R0.9, shown red in Picture 18. The plastic area in Picture 19 is at the root section of the blade and expands over the width of the blade. Force and moment reactions are shown in Picture 20 and Picture 21. Reaction forces and moments were compared to analytically calculated values in Table 8.

Obviously no significant spindle moment was generated, because the loading is uniformly distributed over the blade. Analytical calculations gave good estimations to reaction moments and forces. The maximum reaction force and moment both were about 7% lower than estimated.

Picture 18, Load case 3, Pressure on R0.7-R0.9

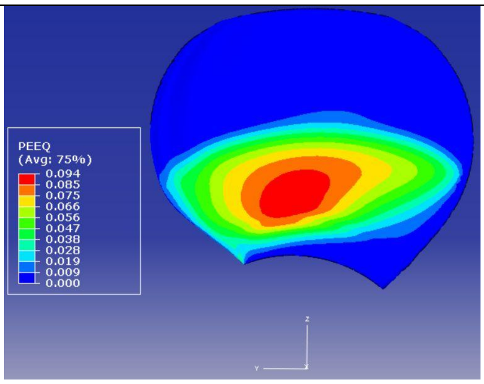

Picture 19, Ship 2 plastic strain at failure U=258mm, Load case 3

Table 8, Load case 3 failure values

Blade, Load case	**Force RF_{max} / Fex**	**Force [%]**	**Bending RM_Y/ M_Y**	**Bending [%]**
Ice, Load case 3	0.97/1.044	92.9%	0.77/0.83	92.7%

where:
RF_{max} = Maximum reaction force in Picture 12
RM_Y = Maximum reaction moment in Picture 20
Fex = Blade failure load, Table 5
M_Y = analytical moment, Table 5
Fex = Blade failure load, Table 5

5.2.7. Load case 3, plots

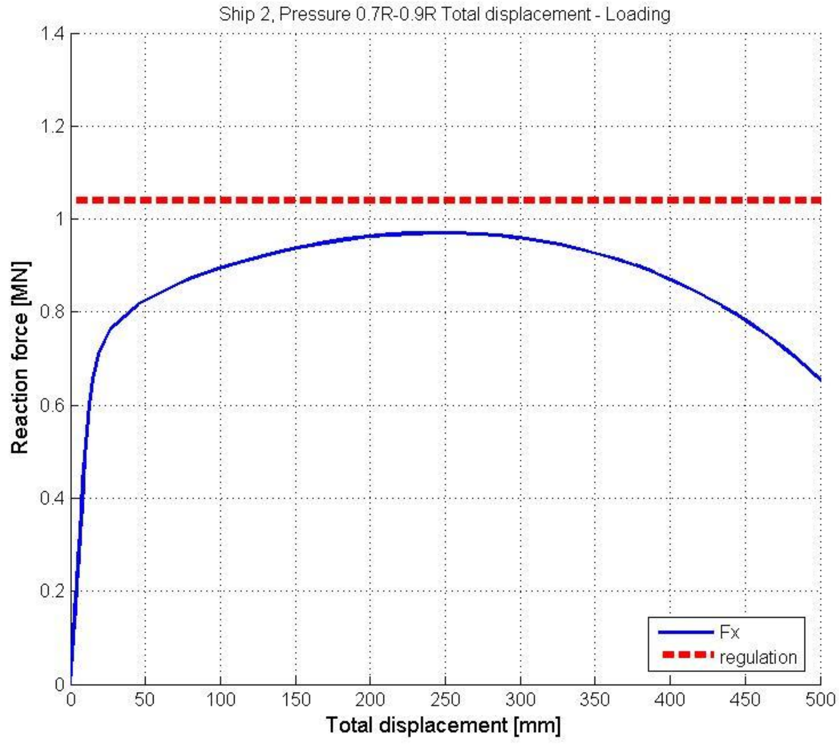

Picture 20, Ship 2 ultimate failure force, Load case 3

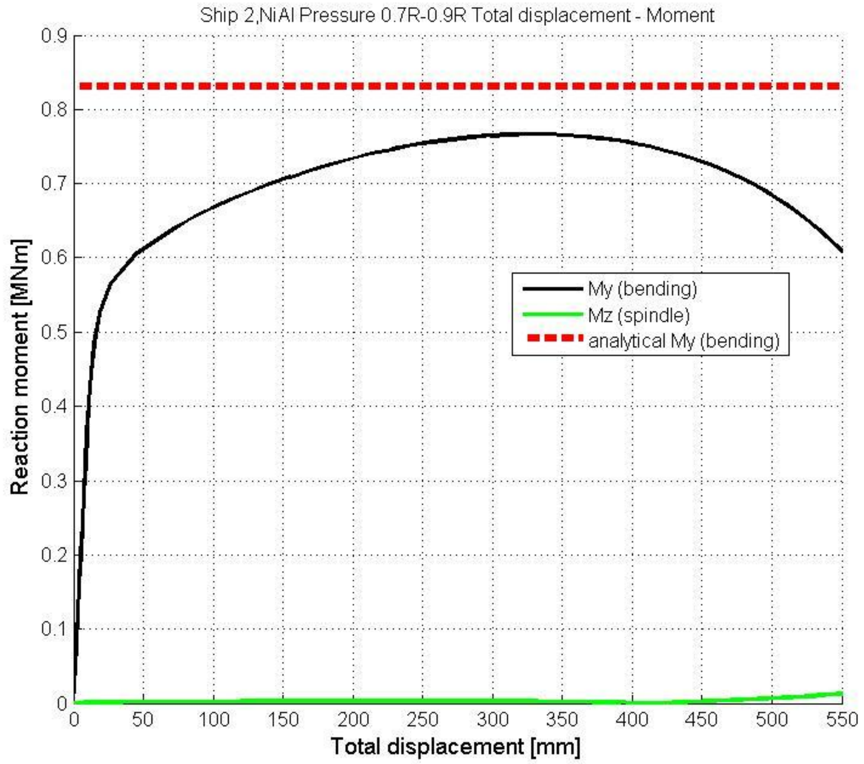

Picture 21, Ship 2 Ultimate bending moment, Load case 3

5.3. Material property validation

In this final case the materials of the studied blades were changed so that ship 1 was calculated with NiAl-Bronze and ship 2 was calculated with steel. All above mentioned load cases were calculated except ship 2 load at trailing edge. Naturally blade failure loads by [1] were also calculated with respective materials, see Table 10. Material properties are listed in Table 9 below.

Table 9, Material properties

Material	**Elastic Modulus E [GPa]**	**Yield/ Ultimate strength [MPa]**	**Poisson constant**	**Elongation [%]**
NiAl-Bronze	123	235/650	0.33	19
Steel	200	520/650	0.3	15

Table 10, Reference loads and moments, B

Blade, Load Case, Material	**Force F_{ex} [MN]**	**Bending M_Y[MNm]**	**Spindle M_Z[MNm]**
Skew, Load case 1,NiAl-Bronze	1.44	2.18	0.84
Skew, Load case 2,NiAl-Bronze	1.44	2.30	0.42
Ice, Load case 1, Seel	1.52	1.12	0.45
Ice, Load case 2, Seel	1.52	1.19	0.25
Ice, Load case 3, Seel	1.52	1.21	0

Where:
F_{ex}= blade failure load by [1], p.38 fomula 6.25
M_Y= analytical propeller shaft bending moment with constant moment arm a, see Picture 4
M_Z= analytical spindle moment with constant moment arm 1/3B or 2/3B specified by load case, see Picture 4

5.3.1. Ship 1

The material of the skewed propeller blade was changed to NiAl-Bronze and blade failure load was calculated using FEM. Load response is shown in Picture 24 and reaction moments in both load cases in Picture 25 and Picture 26. Ultimate reaction forces and calculated blade failure loads on both materials are shown in Table 11. Plastic strain at failure is illustrated and compared in Picture 22
and Picture 23 with both materials and in both load cases.

According to the results propeller blade of ship 1 does not perform as expected by analytical force and moment values if the material is changed. Comparing load cases in Picture 22 and Picture 23 changing material has no significant effect on the orientation of the plastic area. Plastic area is formed at a bigger area than with steel material. Failure load in both load cases is about 30% lower than analytically expected. Propeller shaft bending reaction moments are about 30% lower than expected in both load cases. Analytical estimates for the spindle moment work quite well, especially in load case 2.

Table 11, Ultimate load comparison

Material, Load case	**Force RF_{max} / Fex**	**Force [%]**	**Bending RM_Y/ M_Y**	**Bending [%]**	**Spindle RMz/ Mz**	**Spindle [%]**
Steel, Load case 1	1.975 / 2.10	94.2 %	2.87 / 3.18	90.2%	1.29 / 1.23	102%
Steel, Load case 2	2.034 / 2.10	96.9 %	3.22 / 3.35	96.2%	0.76 / 0.61	124%
NiAl-Bronze, Load case 1	0.99 / 1.44	68.8 %	1.44 / 2.18	66.1%	0.68 / 0.84	81.0%
NiAl-Bronze, Load case 2	1.01 / 1.44	70.1 %	1.63 / 2.30	70.9%	0.40 / 0.42	95.2%

where:
RF_{max} = Maximum reaction force in Picture 8 and Picture 24
RM = Maximum reaction moments in Picture 9, Picture 10, Picture 25 and Picture 26
M_Y = analytical moment, Table 5 and Table 10
M_Z = analytical moment, Table 5 and Table 10
Fex = Blade failure load, Table 5 and Table 10

Ship 1, Load at 2/3 (NiAl-Bronze)	**Ship 1, Load at 2/3 (Steel)**
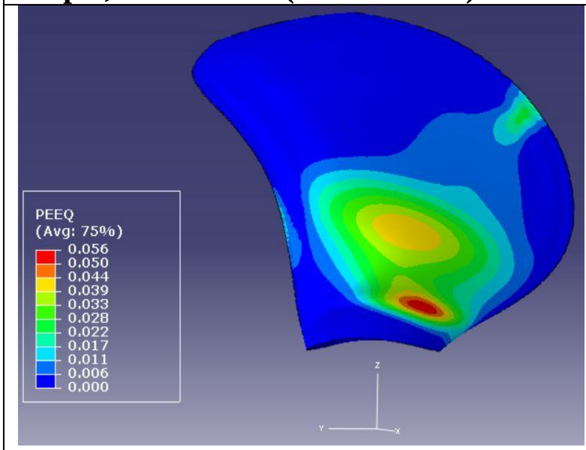	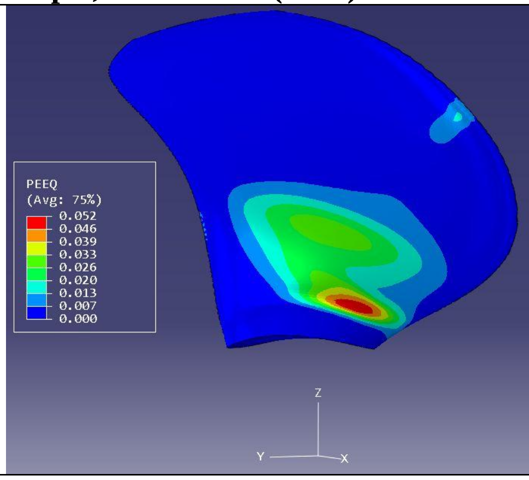
A: Plastic strain at failure U=305mm	**B:** Plastic strain after failure U=200mm
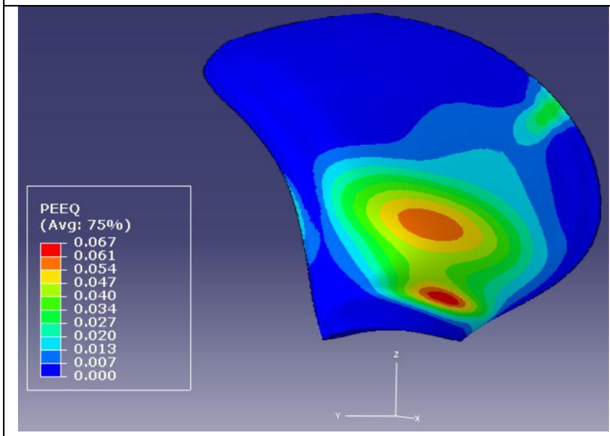	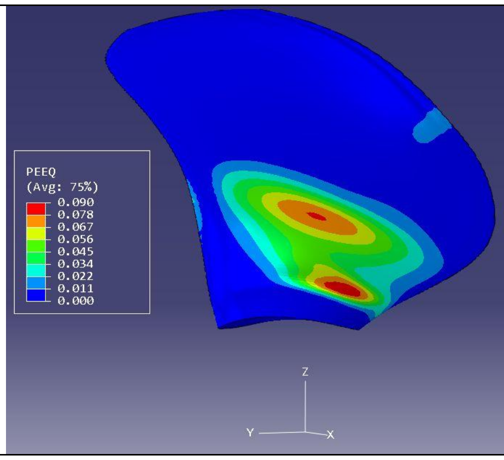
C: Plastic strain at failure U=305mm	**D:** Plastic strain after failure U=400mm

Picture 22, Ship 1 Comparison of plastic deformation, Load case 1

<table>
<tr><td>Ship 1, Load at 1/3 (NiAl-Bronze)</td><td>Ship 1, Load at 1/3 (Steel)</td></tr>
<tr><td>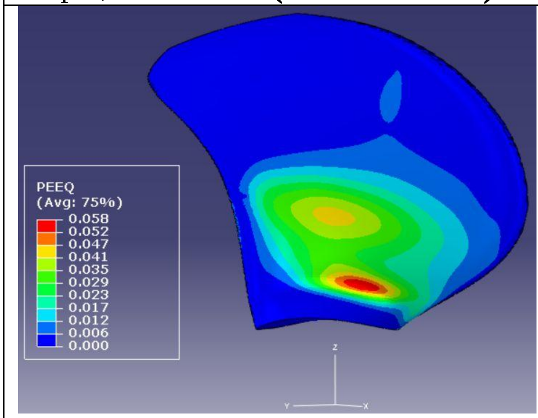
</td><td>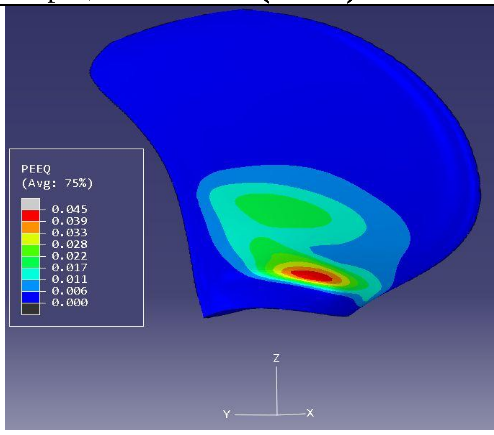
</td></tr>
<tr><td>A: plastic strain at failure U=337mm, Max strain ≈5.8%</td><td>B: Plastic strain at failure, U≈200mm, Max strain≈4.5%</td></tr>
<tr><td>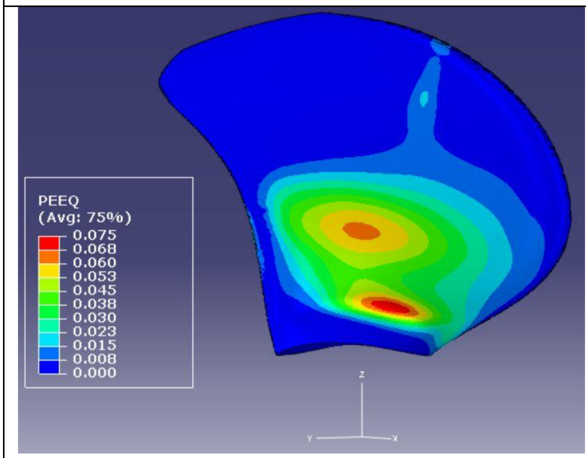
</td><td>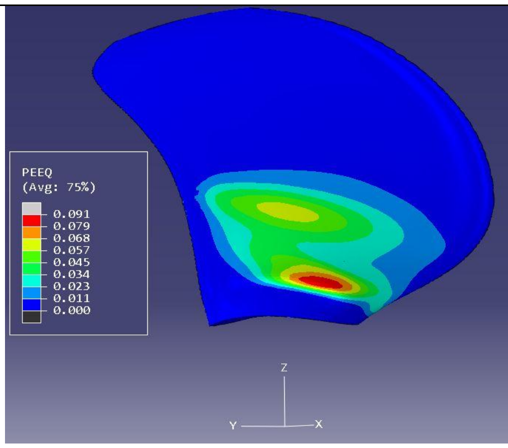
</td></tr>
<tr><td>C: plastic strain at U=468mm, , Max strain ≈7.5%</td><td>D: Plastic strain propagation U≈400, Max strain ≈9.1%</td></tr>
</table>

Picture 23, Ship 1 Comparison of plastic deformation, Load case 2

5.3.2. Ship 1, plots

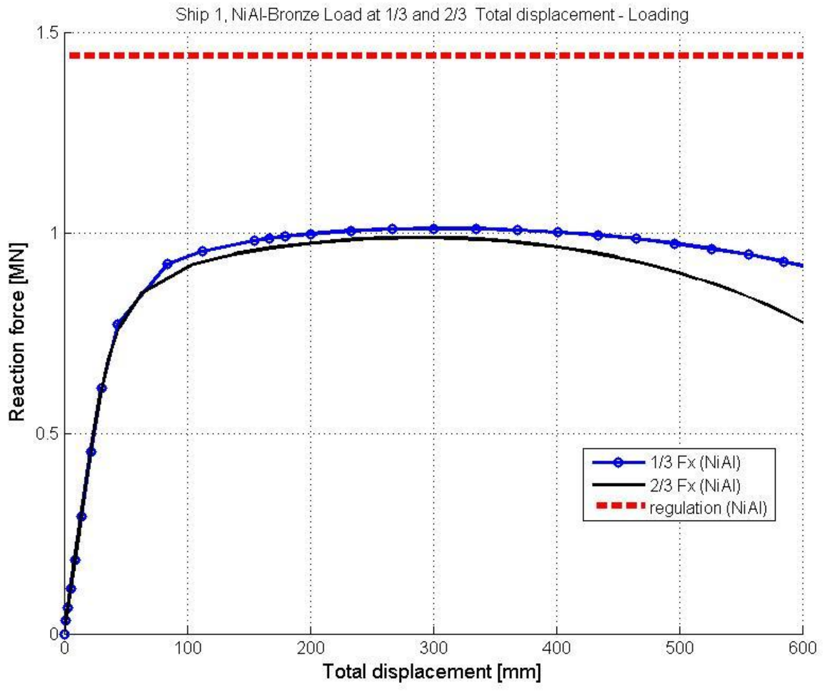

Picture 24, Ship 1 Reaction force, NiAl-Bronze

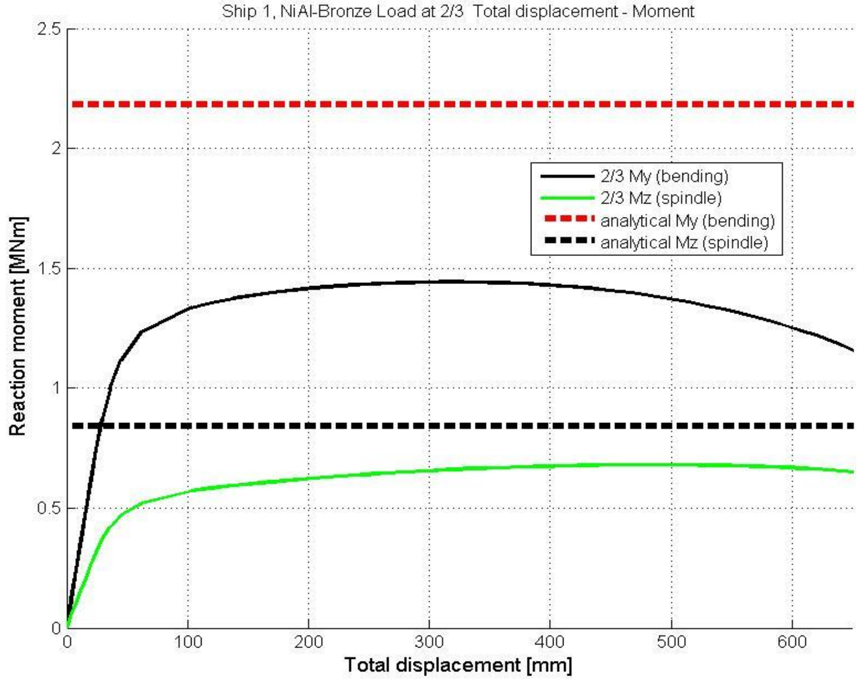

Picture 25, Ship 1 Reaction moments, NiAl-bronze

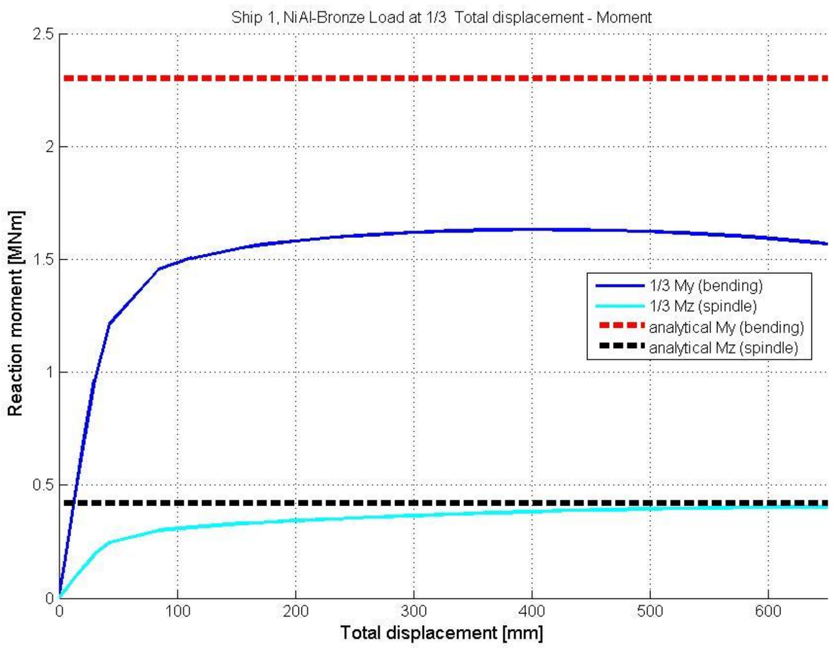

Picture 26, Ship 1, Reaction moments, Load case 2, NiAl-Bronze

5.3.3. Ship 2

The material of ship 2 was changed form NiAl-Bronze to steel and blade failure load was calculated in three load cases using FEM. Response in load cases 1 and 2 are shown in pictures 27 to 29 and load case 3 response is shown in Picture 30 and Picture 31. Plastic areas in load cases 1, 2 and 3 are examined in Picture 32 to 34. Maximum reaction forces and moments are compared to analytical values in Table 12.

1.1.1.1 Load cases 1 and 2

The blade failure load for steel in Picture 27 does not reach analytically calculated value for both load cases. Failure in load case 1 occurs some 30% lower than analytically expected and both reaction moment components do not reach expected values. Plastic deformation is generated locally near the loaded area. In load case 2 however analytical calculations give fairly good estimates for spindle torque and bending moment of the propeller shaft. Still plastic deformation occurs locally near the loaded area. Changing material has no significant effect on the orientation of the plastic area.

1.1.1.2 Load case 3

Ultimate reaction force and bending moment values exceed the analytical estimations by some 10 to 15%. Again spindle moment is not significantly generated. Plastic deformation is generated at the root of the blade and the area expands over the width of the blade.

Table 12, Ship 2, Ultimate load comparison

Material, Load case	**Force RF_{max}/Fex**	**Force [%]**	**Bending RM_Y/ M_Y**	**Bending [%]**	**Spindle RMz/ Mz**	**Spindle [%]**
NiAl-Bronze, Load case 1	0.555/1.044	53.2%	0.39/0.77	50.6%	0.17/0.31	54.8%
NiAl-Bronze, Load case 2	0.713/1.044	68.3%	0.55/0.82	67.1%	0.14/0.16	87.5%
NiAl-Bronze, Load case 3	0.97/1.044	92.9%	0.77/0.83	92.7%	0, *not relevant*	
Steel, Load case 1	1.05/1.52	69.1%	0.73/1.12	65.2%	0.32/0.45	71.1%
Steel, Load case 2	1.36/1.52	89.5%	1.04/1.19	87.4%	0.24/0.25	95.6%
Steel, Load case 3	1.75/1.52	115%	1.32/1.21	109%	0, *not relevant*	

where:
RF_{max} = Maximum reaction force in Picture 8 and Picture 24
RM = Maximum reaction moments in Picture 9, Picture 10, Picture 25 and Picture 26
M_Y = analytical moment, Table 5 and Table 10
M_Z = analytical moment, Table 5 and Table 10
Fex = Blade failure load, Table 5 and Table 10

5.3.4. Ship 2, plots

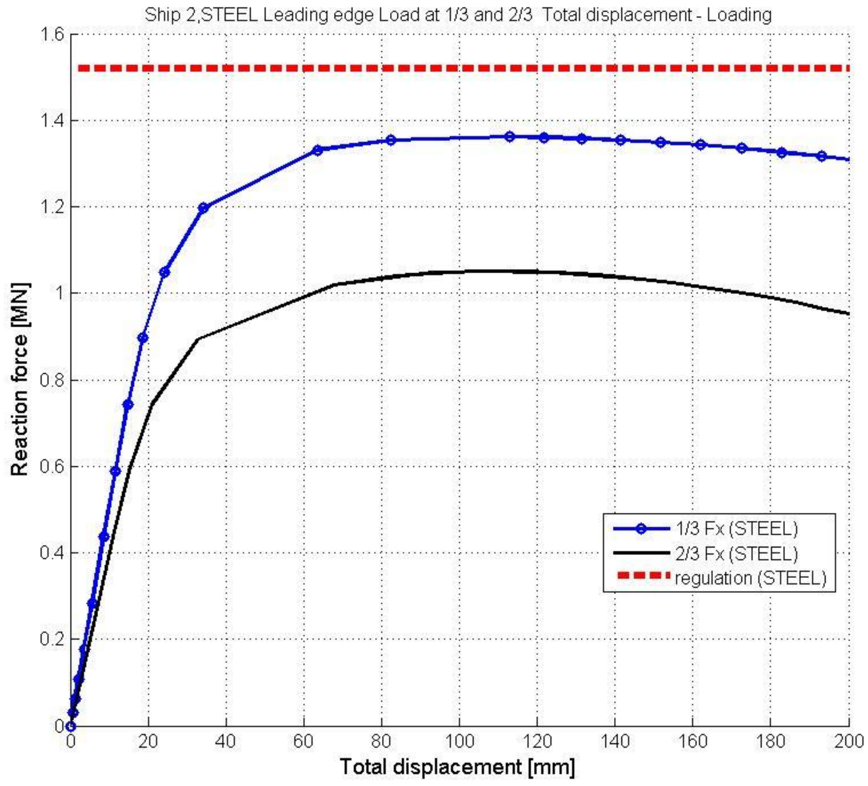

Picture 27, Ship 2 Reaction forces, Steel

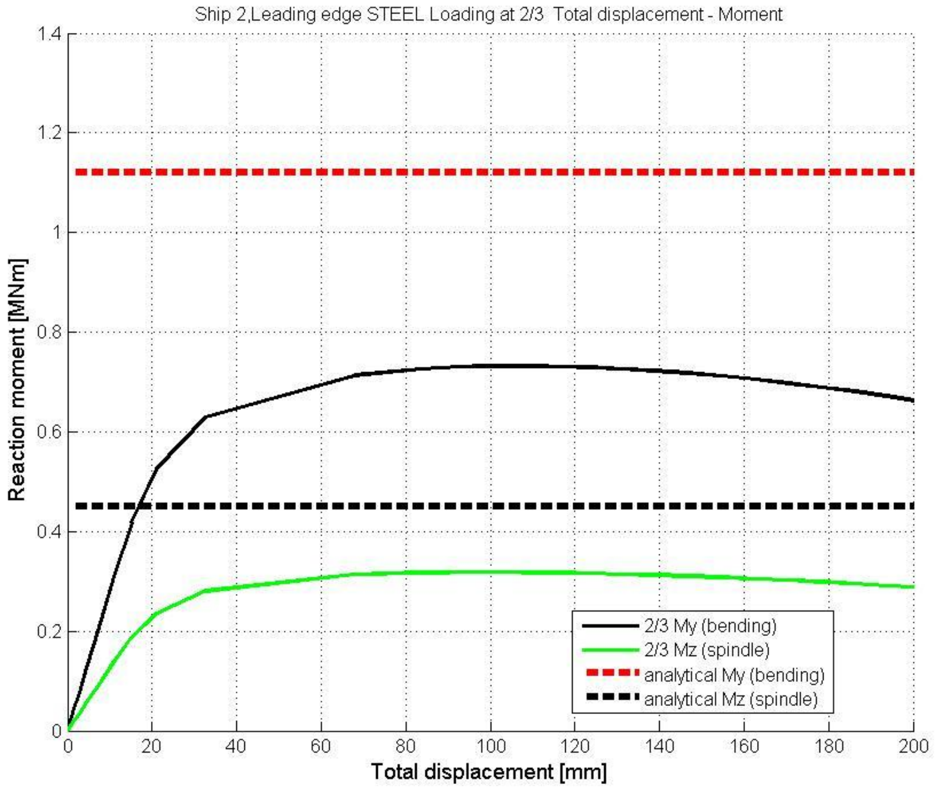

Picture 28, Ship2 Reaction moments, Steel

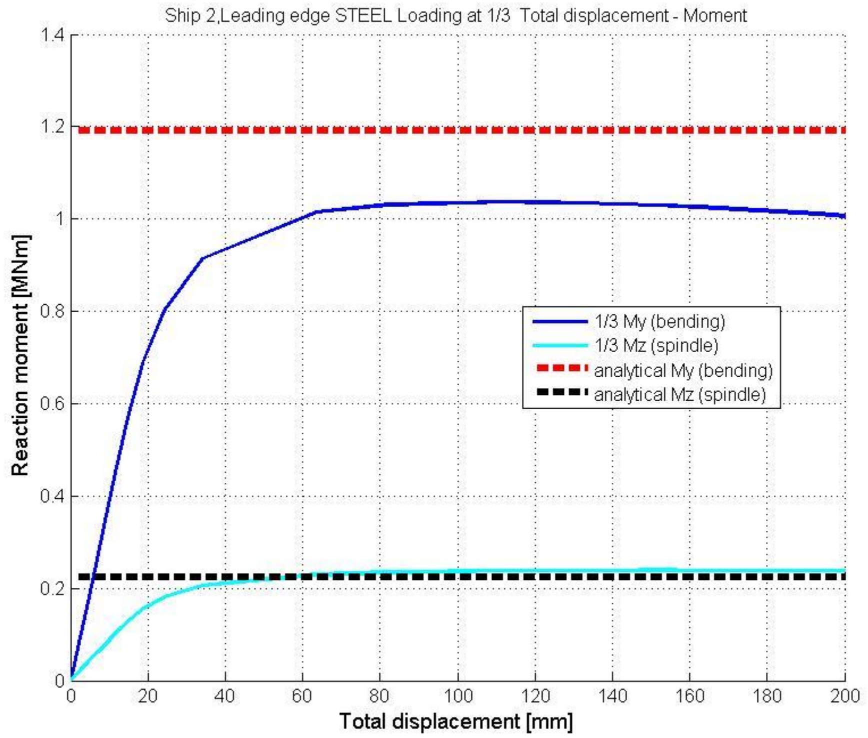

Picture 29, Ship 2 Reaction moments, Steel load case 2

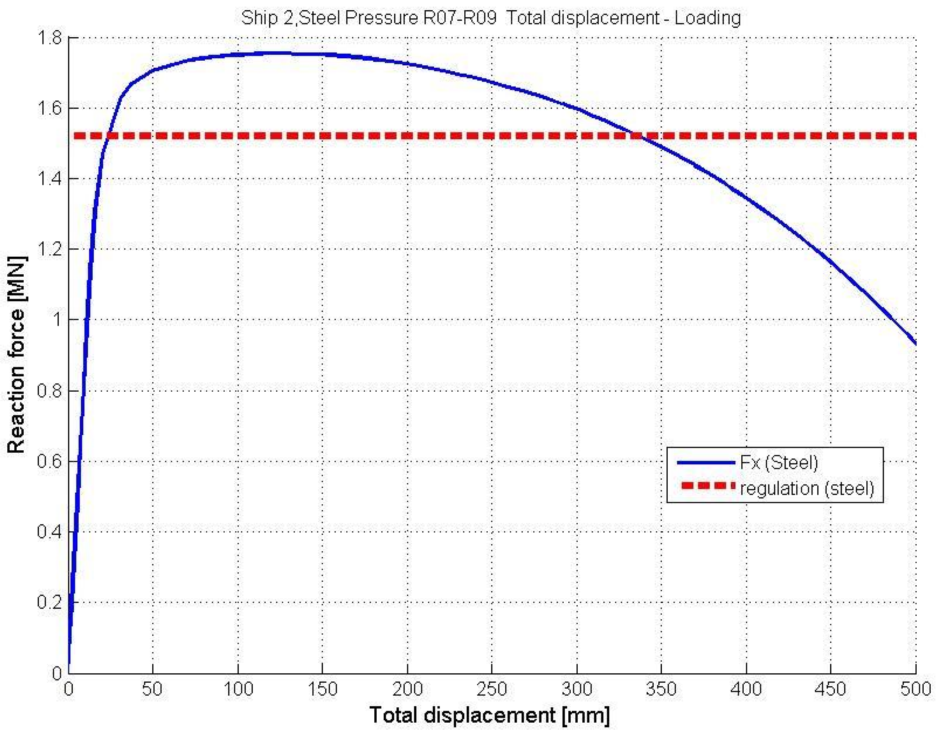

Picture 30, Ship 2 force response, load case 3, Steel

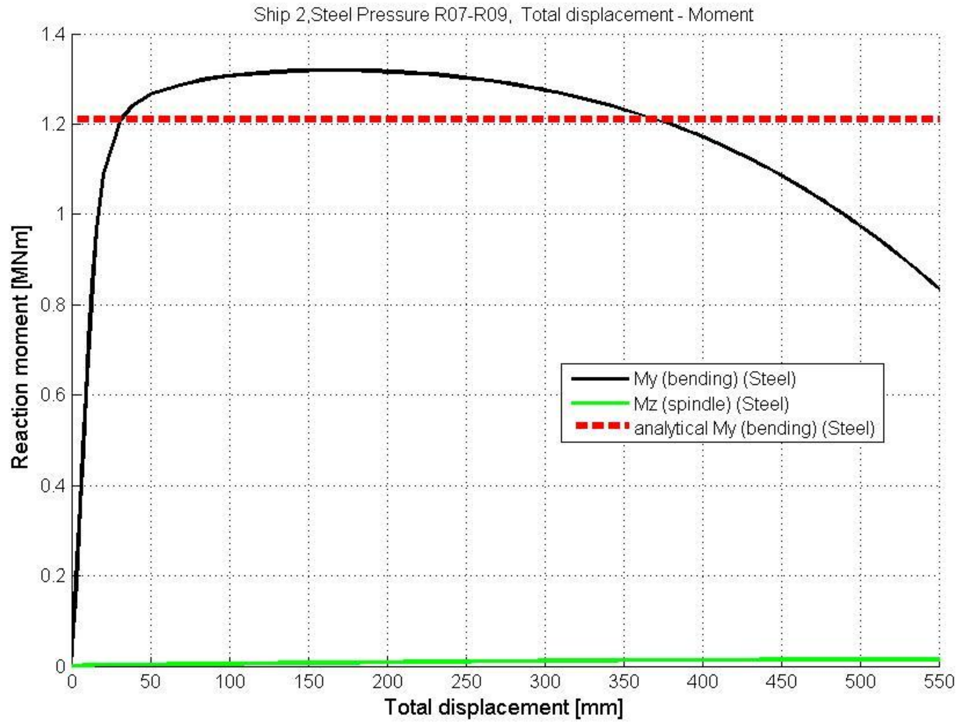

Picture 31, Ship 2, reaction moment, load case 3, Steel

<table>
<tr><th>Ship 2 Load at 2/3 (Steel)</th><th>Ship 2 Load at 2/3 (NiAl-Bronze)</th></tr>
<tr><td>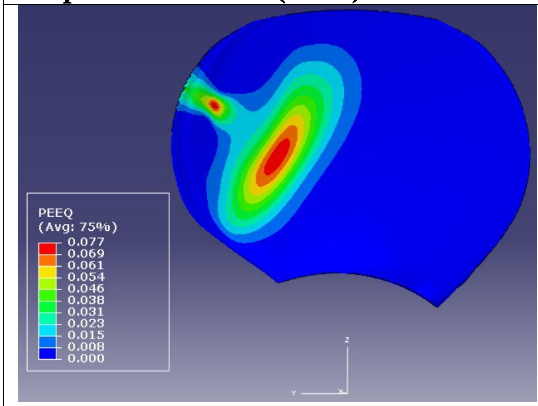
</td><td>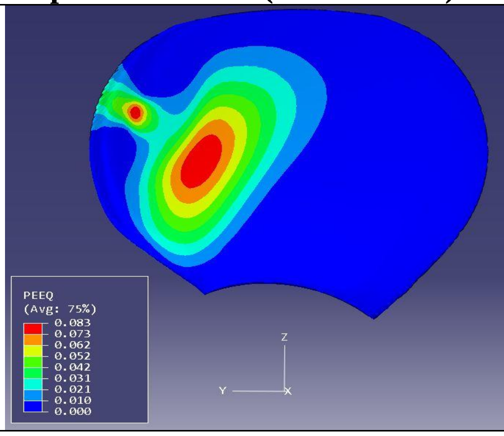
</td></tr>
<tr><td>A: Plastic strain at failure, U=108mm, max strain=7,7%</td><td>B: Plastic strain at failure, U=150mm, max strain=8,3%</td></tr>
<tr><td>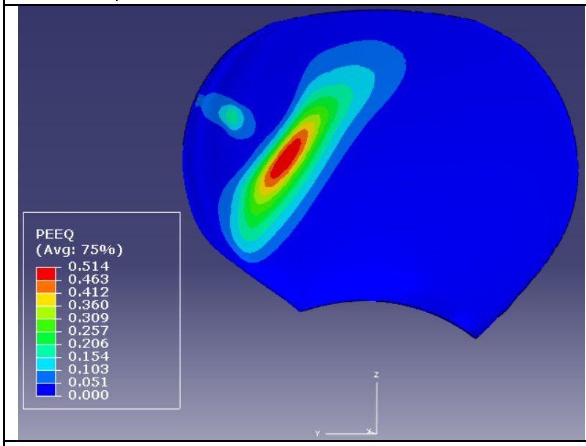
</td><td>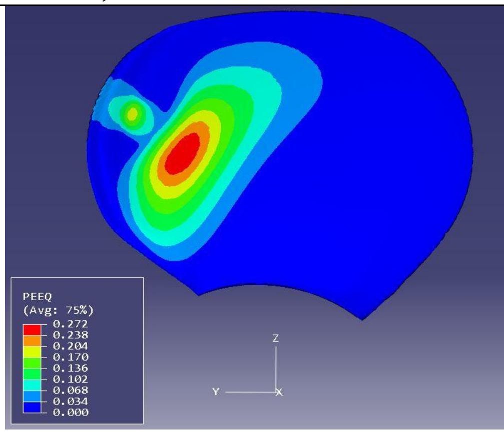
</td></tr>
<tr><td>C: Plastic strain after failure, U=350mm</td><td>D: Plastic strain after failure U=350mm</td></tr>
</table>

Picture 32, Ship 2, Comparison of plastic deformation, Load case 1

Ship 2 Load at 1/3 (Steel)	**Ship 2 Load at 1/3 (NiAl-Bronze)**
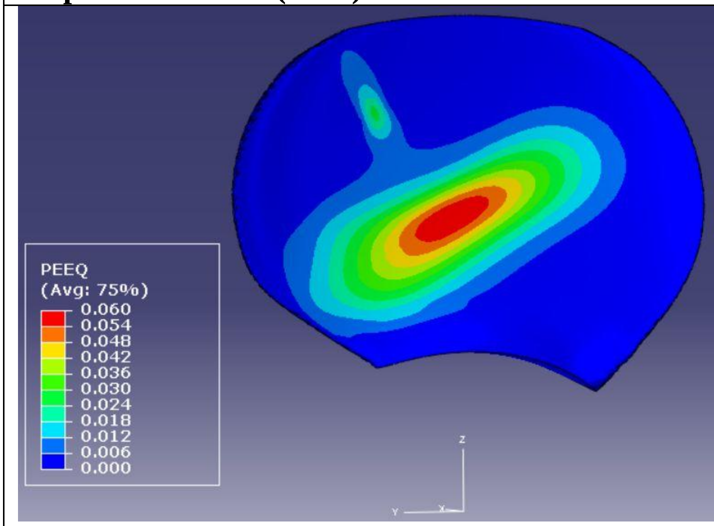 **A:** plastic strain at failure U=113mm, Max strain =6%	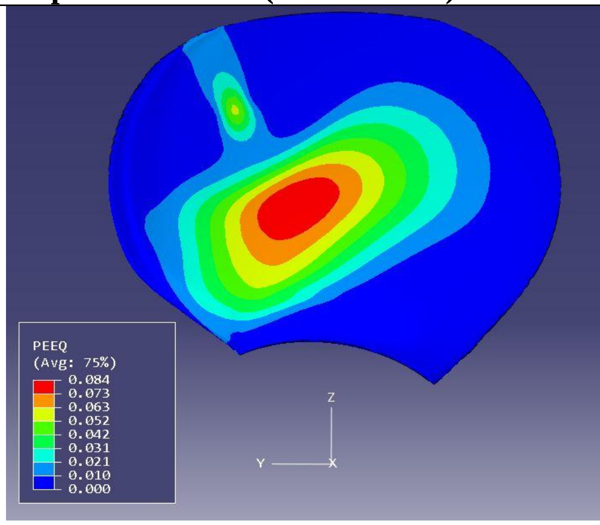 **B:** plastic strain at failure U_{max}=202mm, Max strain =8.4%
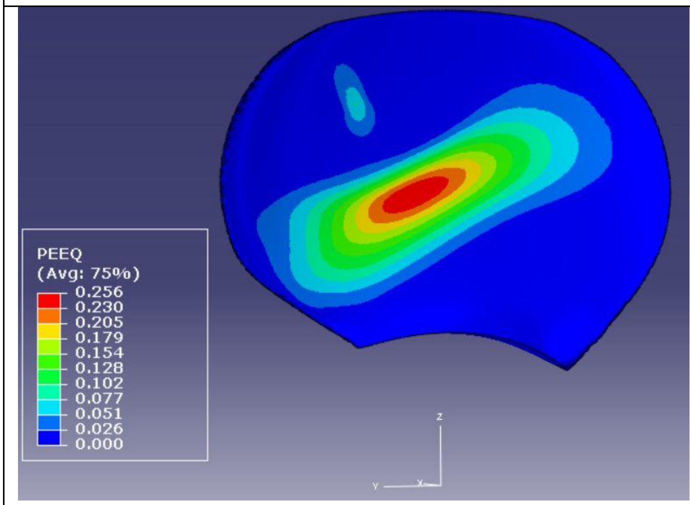 **C:** plastic strain at U=348mm	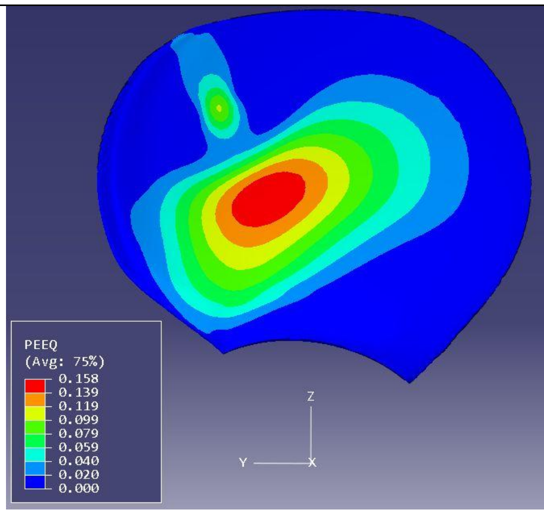 **D:** plastic strain at U=350mm

Picture 33, Ship 2, Comparison of plastic deformation, Load case 2

Ship 2, Load case 3, Steel	**Ship 2, Load case 3, NiAl-Bronze**
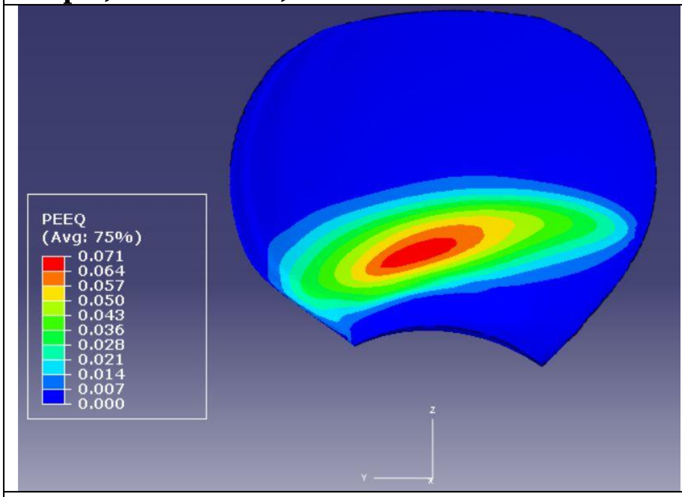	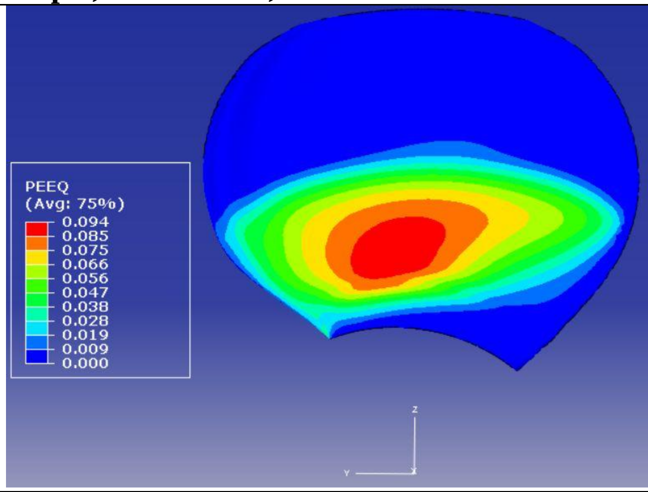
A: Plastic strain at failure U=258mm, max strain 7.1%	**B:** Plastic strain at failure, U=124mm, max strain 9.4%

Picture 34, Ship 2 plastic areas at failure, load case 3

6. Conclusions

Ship1, Skew: Blade failure load estimation is realistic. No need to change the Ice Class Regulations rule for blade failure load. If spindle arm would be changed to 1/3, this would result in too low spindle torque estimates.

Ship 2, Ice blade: Blade failure load calculation does not work for blades of big EAR (Expanded blade area ratio). The Ice Class Regulations rule for the blade failure load assumes that the plastic hinge is formed at the blade root section. According to the numerical studies this assumption is not valid for this kind of propeller geometry thus leading to much smaller blade failure loads than the regulations predict.

7. Appendix

7.1. A: Calculation model validation

The geometry of the real propeller blades is too complex to be meshed with hexagonal elements, so the propellers are meshed with 10-noded parabolic tetrahedron elements. To confirm the relevance of the blade FE-models an element type validation was conducted. A test model is used to compare the results of different element types and to choose a sufficient element density over the thickness of the plate.

The propeller blade is simplified to a plate model, seen in Picture 36. To make calculations faster the plate was not fully modelled, instead three element layers broad model was made to represent the plate midsection, Picture 35. Dimensions of the test model are shown in Table 13. The thin model is restricted by boundary conditions to match the physical plane-strain condition of the plate in pure bending. Isotropic steel was used as material and strain hardening was modelled with a bilinear material model.

Table 13, Test model dimensions

model	length (x)	width (z)	Plate thickness (y)
Test model full scale	900mm	1200mm	100mm
Thin model	900mm	3mm	100mm

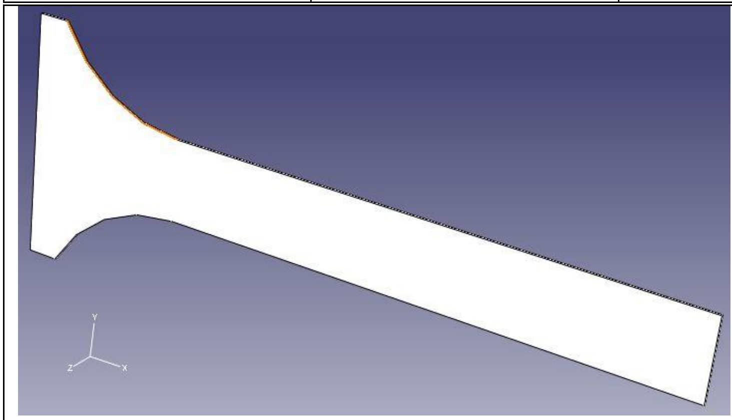

Picture 35, Thin test model

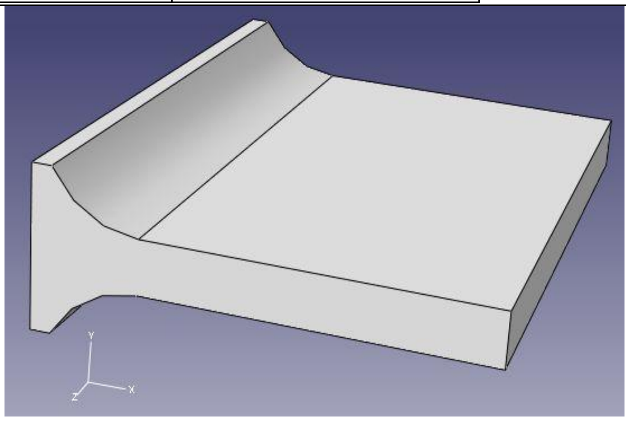

Picture 36, Test model plate

1.1.2 Meshing, loading and boundary conditions

The test model was meshed with following element densities: i= 4, 6, 8, and 16 elements over the thickness (y direction) of the plate. This element density is marked with index i=”element density”. In the comparisons following Abaqus element types were studied:

- Hexagonal C3D20, fully integrated, parabolic
- Tetrahedron C3D10, fully integrated, parabolic

The C3D20 element represents the more accurate and well behaving element, which typically gives accurate results with less computational cost. The results of the tetrahedron C3D10 elements are compared to C3D20 results.

Loading was applied to the free end of the plate. The load was given as a pressure of 24 MPa in the area seen in red in Picture 37. This area varies according to element size. The model was rigidly constrained at the root section, yellow cross seen in Picture 37.

Picture 37 illustrates the tetrahedron mesh of 8 elements over the thickness of the plate. After the first test run the plastic region due to bending was discovered to appear in the region of the elements shown red in Picture 38. Data from the mentioned elements is discussed further in this report. The end tip displacement (U) is measured from the tip nodes at the free end of the plate.

The following quantities were compared:

- Pressure load – displacement U
- U - Mises stress at Compression on surface
- U - plastic strain components at compression on the surface of the plastic area
- U - plastic strain components at compression near neutral axis

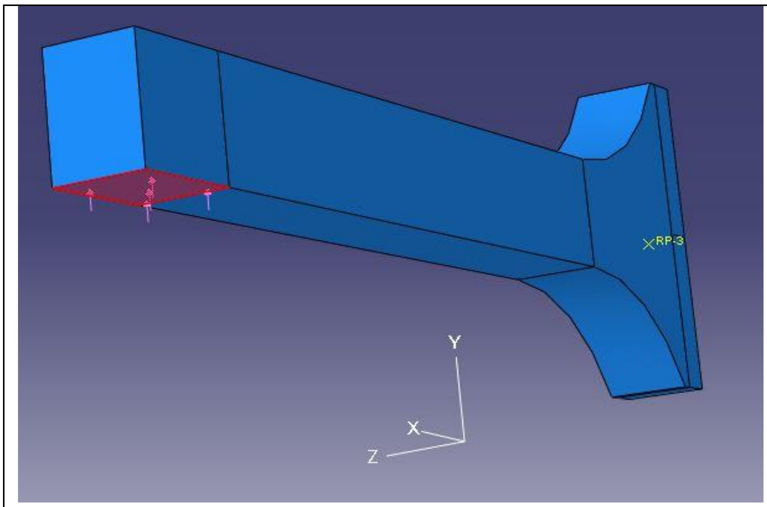

Picture 37, Loaded area

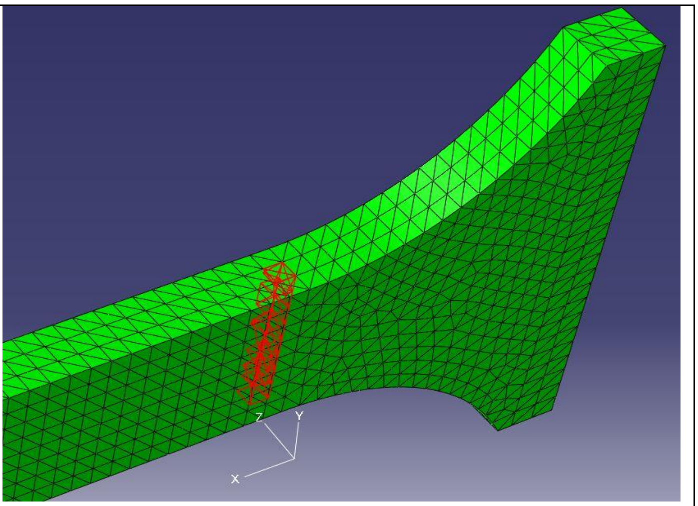

Picture 38, Elements at plastic region

1.1.3 Results

The plastic strain distribution at particular pressure load of the plate model is shown in Picture 39 and Picture 40. Areas shown in dark have no plastic deformation. A plastic hinge is formed in the coloured area in all models. Similar distributions in Picture 39 and Picture 40 indicate adequate performance of tetrahedron elements.

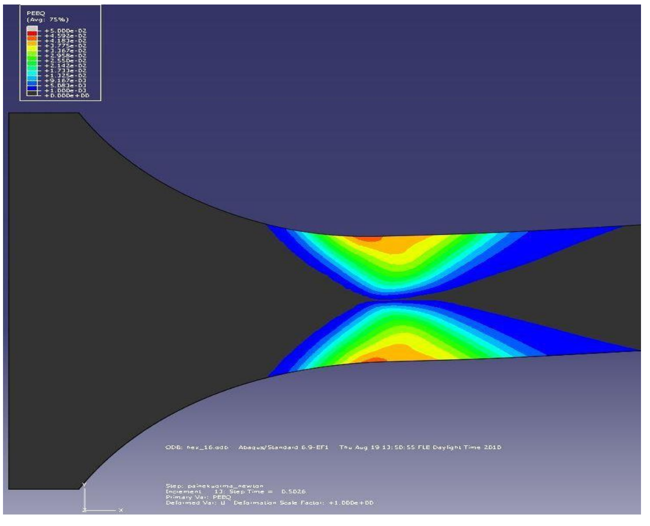

Picture 39, Deformation and plastic strain, hexagonal elements, 16 elements across the thickness

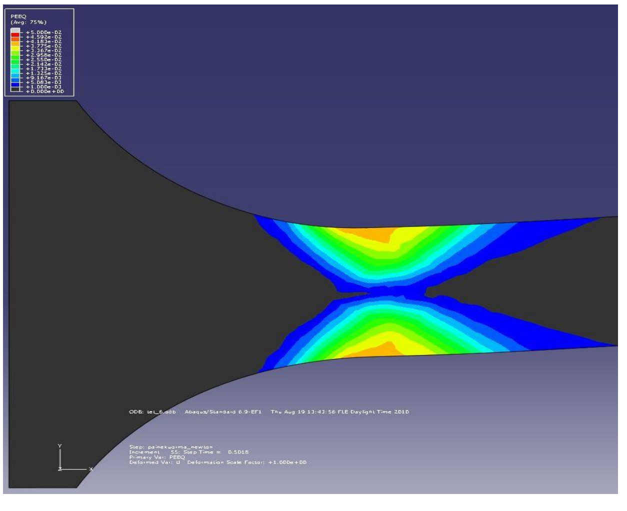

Picture 40, Deformation and plastic strain, tetrahedral elements, 8 elements across the thickness

The global response of the test models with the studied element densities is seen in Picture 41. Even i=4 model is able to describe the behaviour of the test model in bending and the yielding point is realistic. Abaqus bilinear material model for steel is behaving well. The initial rapid rise of pressure load indicates loading in the elastic region of the material and yielding begins at around 11 MPa pressure.

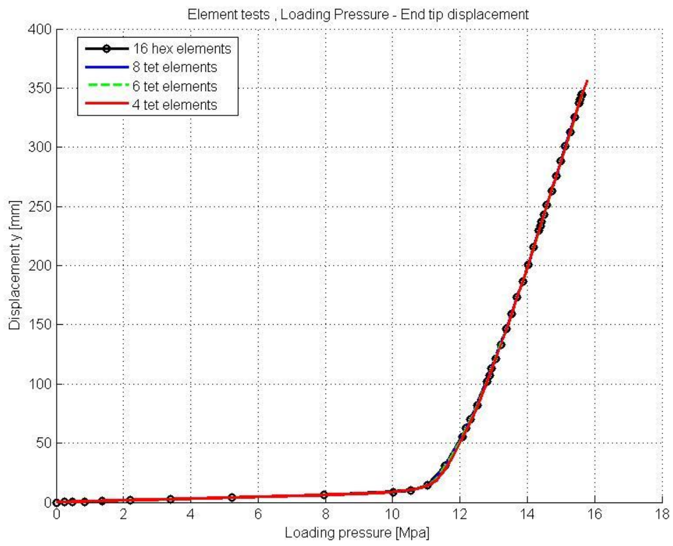

Picture 41, Global response

Von Mises stress at the surface of the plastic area is shown in Picture 42. Hex 16 model performs best and stress after yielding point is calculated correctly. All tetragonal models shoot over the yielding point, but this has no effect on the overall displacement response and the problem might be solved by reducing the applied load increment.

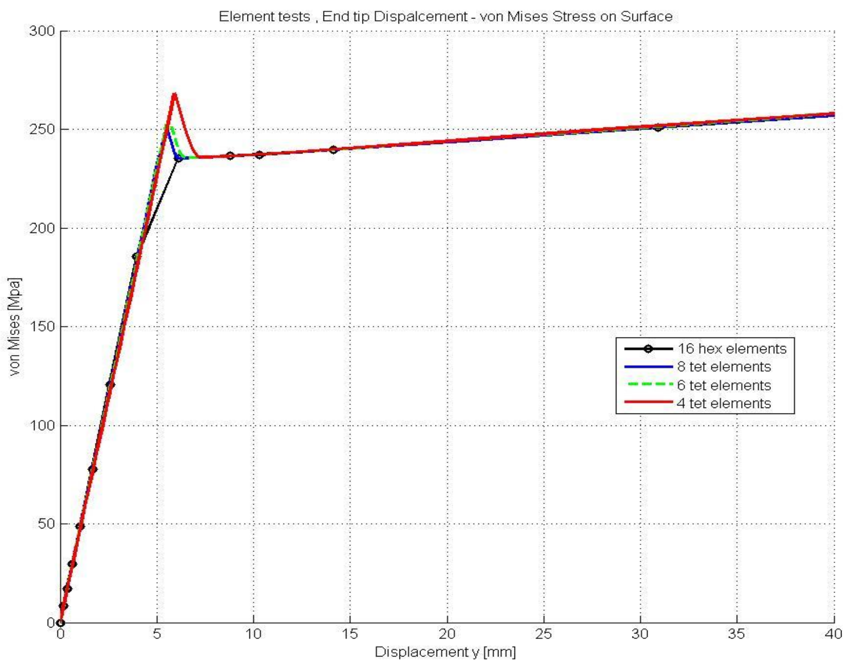

Picture 42, Testmodel material behaviour

Plastic strain at the surface of the plastic region versus the plate tip displacement was very similar in all models. Picture 8 illustrates the behaviour of the plastic strain components at the compression side of the plate at a distance of 25 mm from the surface. All models except the coarse i=4 tetrahedron model converge to the result of hexagonal i=16.

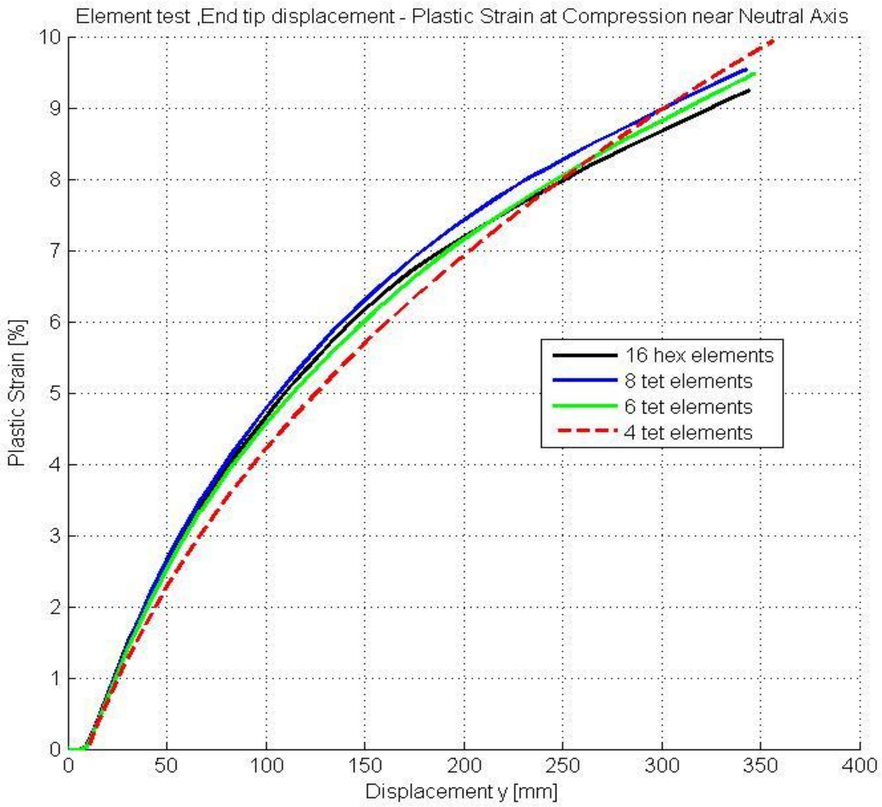

Picture 43, Plastic behaviour

The overall plastic behaviour of the test models is compared in Table 14 below. At a specific load increment of 12MPa the amount of plastic elements is calculated. The tetrahedron model with four elements across the plate thickness predicts a larger plastic area than the other models due to the much bigger element size.

Table 14, Plastic elements

Test model	**No. of plastic elem./ Total elem.**	**Plastic elements**	**Pressure**
Hex 16	1101/8793	12,5 %	12,02 MPa
Tet 8	2216/15320	14,5 %	12,00 MPa
Tet 6	1331/9374	14,2 %	12,00 MPa
Tet 4	686/4195	16,4 %	12,00 MPa

1.1.4 Conclusions

According to this study no less than 6 tetrahedron elements over the thickness of the propeller blade should be used to achieve an adequate resolution in the propeller blade failure load analysis. The real propeller models are meshed with 8-10 elements across the cross section in the plastic region and its surroundings thus being able to predict the failure load reliably.

References

1. Finnish Maritime Administration Bulletin 10/10.12.2008, Ice Class Regulations 2008 (Finnish-Swedish Ice Class Rules), No. 2530/30/2008, ISSN 1455-9048